

PARTICLE INTERACTIONS IN OSMOPHORESIS

H. J. KEH and F. R. YANG

Department of Chemical Engineering, National Taiwan University, Taipei, Taiwan, R.O.C.

(Received 6 June 1991; in revised form 16 January 1992)

Abstract—An exact analytical study is presented for the osmophoretic motion of two spherical vesicles in a constant solute concentration gradient arbitrarily oriented with respect to the line of vesicle centers. The vesicles may be formed from different semipermeable membranes, contain arbitrary solutes and have unequal radii. The appropriate equations of conservation of solute species and fluid momentum are solved in the quasisteady limit using spherical bipolar coordinates and the translational and angular velocities of the vesicles are calculated for various cases. The interaction between vesicles can be strong and peculiar when the surface-to-surface spacing gets close to zero. The influence of the interaction, in general, is stronger on the smaller vesicle than on the larger one. For the osmophoresis of two identical vesicles along their line of centers, both migrate slower than the velocity they would possess if isolated. On the contrary, for the case of two identical vesicles undergoing osmophoresis normal to their line of centers, they migrate faster than their undisturbed velocity except when the two vesicles are very close together. A comparison between our exact results for osmophoretic velocities and those evaluated from asymptotic formulas obtained using a method of reflections is made for a case of two identical vesicles. The asymptotic formulas for the vesicle velocities up to $O(r_{12}^{-6})$, where r_{12} is the center-to-center distance between the vesicles, are found to underestimate (for the axisymmetric osmophoresis) or to overestimate (for the transverse motion) the effect of particle interactions; the error can be significant when the vesicle surfaces are less than half the vesicle radius apart. Our numerical results for the interaction between two vesicles are also used to find the effect of the volume fraction of vesicles on the average osmophoretic velocity in a bounded dispersion.

Key Words: osmophoresis, semipermeable vesicle, particle interaction, spherical bipolar coordinates, effect of volume fraction.

INTRODUCTION

The existence of a solute concentration gradient in an unbounded solvent does not by itself generate an appreciable volume flow. However, when two solutions differing in concentration are separated by a semipermeable membrane, i.e. a membrane that permits the passage of solvent but not of solute, it is observed that solvent at the side of lower concentration tends to pass through the membrane into the solution of higher concentration, and thereby dilute it. This behavior is called osmosis. The osmotic flow of solvent can be prevented by applying a pressure to the solution of high concentration which is greater than the pressure on the solution at the other side by an amount equal to the difference in osmotic pressure between the two solutions.

The fluid velocity normal to a semipermeable membrane is usually characterized by the equation

$$v_n = L_p(\Delta\Pi - \Delta P), \quad [1]$$

where ΔP and $\Delta\Pi$ are the differences in mechanical and osmotic pressures across the membrane, respectively, and L_p is the hydraulic coefficient which is a constant for a given membrane and solvent. For an ideal solution (with very low solute concentration), the osmotic pressure Π is related to the solute concentration C by the van't Hoff law:

$$\Pi = RTC, \quad [2]$$

where R is the gas constant and T is the absolute temperature. In general, Π is a non-linear function of C at fixed temperature.

When a vesicle, which is a body of fluid surrounded by a semipermeable membrane, is placed in a solution of uniform, but perhaps different, concentration of impermeable solute, the membrane interchanges solvent between the internal and external solutions until an equilibrium condition is reached such that $P_{in} - P_{out} = \Pi_{in} - \Pi_{out}$. On the other hand, if the external concentration is non-uniform, one pole of the vesicle sees a higher solute concentration (and hence a higher osmotic

pressure) than the opposite pole. According to [1], a driving force causes solvent to cross the vesicle's membrane from inside to outside at the high concentration pole, and from outside to inside at the low concentration pole. The vesicle thus acts as a micro-engine, sucking fluid into it on one side and ejecting fluid on the other, thereby advancing toward regions of low concentration. This movement of the vesicle by osmotic force is termed "osmophoresis" (Gordon 1981; Anderson 1983) and provides a mechanism for the motion of biological cells in response to chemical gradients, a phenomenon known as "chemotaxis" (Devreotes & Zigmond 1988).

The osmophoresis of a spherical or ellipsoidal vesicle with a very thin membrane through a constant solute gradient has been examined theoretically in considerable detail by Anderson (1983, 1984). He calculated the terminal velocity of a spherical vesicle of radius a placed in an unbounded fluid of viscosity η , with a linear concentration distribution $C_\infty(\mathbf{x})$ far away from the vesicle, for a quite general case. If the semipermeable vesicle is sufficiently small that the effects of inertia and the convection of solute species are negligible, its velocity $\mathbf{U}^{(0)}$ is related to the uniform concentration gradient ∇C_∞ by the expression

$$\mathbf{U}^{(0)} = -\frac{1}{2}aL_pRT\left(1 + \bar{\kappa} + \frac{\kappa}{2} + 10\lambda\right)^{-1}\nabla C_\infty, \quad [3]$$

with dimensionless parameters

$$\kappa = \frac{aL_pRTC_\infty(\mathbf{x}_0)}{D}, \quad [4a]$$

$$\bar{\kappa} = \frac{aL_pRT\bar{C}}{\bar{D}} \quad [4b]$$

and

$$\lambda = \frac{\eta L_p}{a}, \quad [4c]$$

where \bar{D} and D are the solute diffusion coefficients inside and outside the vesicle, respectively, \bar{C} is the average internal concentration of solute and \mathbf{x}_0 denotes the position of the vesicle center. For most physically realistic systems, the last term in the parentheses in [3] is orders of magnitude smaller than the other terms and may be safely neglected (Anderson 1983). The van't Hoff expression [2] was used in deriving [3]; if it is not valid, then RT must be replaced by $\partial\Pi/\partial C$, evaluated at $C_\infty(\mathbf{x}_0)$ in [3] and [4a] and at \bar{C} in [4b].

Ignoring the λ term, two extreme cases of [3] give different mechanisms for the movement of the vesicle. At small aL_p or low solute concentration ($\bar{\kappa} + \kappa/2 \ll 1$), $\mathbf{U}^{(0)} \approx -\frac{1}{2}aL_pRT\nabla C_\infty$ and the velocity is determined solely by the vesicle's properties and the osmotic gradient. However, at large aL_p or high solute concentration ($\bar{\kappa} + \kappa/2 \gg 1$), $\mathbf{U}^{(0)} \approx -(1 + 2\bar{\kappa}/\kappa)^{-1}D\nabla \ln C_\infty$ and the velocity becomes independent of the physical properties of the vesicle (membrane). Equation [3] shows that the vesicle always moves toward regions of lower C_∞ , no matter what the relative values of C_∞ and \bar{C} are; i.e. there exists no equilibrium position as long as ∇C_∞ is non-zero. Loading the inside of the vesicle with solute has a retarding effect on its velocity.

In real situations of osmophoresis, vesicles are not isolated and will move in the presence of neighboring vesicles and/or boundaries. For example, the presentation of immune cells (such as phagocytes) moving in chemotactic response to the specified gradients released by various invading pathogens to reach a target in the tissue matrix (such as on the lung surface) requires cell-target and cell-cell contact (Charnick & Lauffenburger 1990). Also, the most commonly used experimental assay for bacterial chemotaxis is the capillary assay, in which cellular transport due to chemokinetic effects occurs in capillary tubes (Berg & Turner 1990). Using a method of reflections, Anderson (1986) analyzed osmophoretic motions of a spherical vesicle with $\kappa = \bar{\kappa} = \lambda = 0$ in the proximity of another identical vesicle and along the axis of a long circular pore. Corrections to [3] due to the presence of another vesicle or the pore wall were determined in a power series of $1/r_{12}$ up to $O(r_{12}^{-6})$, where r_{12} is the center-to-center distance between the vesicles or the distance of the vesicle center from the wall. Anderson's (1986) results illustrate that the characteristics of the particle-interaction and boundary effects on osmophoresis are quite different from those for

sedimentation (Happel & Brenner 1983) and other “phoretic” motions such as electrophoresis (Keh & Anderson 1985; Chen & Keh 1988).

For the case of two vesicles undergoing osmophoresis with a large to moderate separation, the power-series results from one or two reflections describe the particle interactions adequately. However, when the vesicles are closer together, higher order interactions become significant and the leading terms in the asymptotic solution result in a poor description of the particle-interaction effect. The object of this paper is to obtain an exact solution to the quasisteady problem of osmophoresis of two arbitrarily oriented spherical vesicles. The vesicles may have different semipermeable membranes, hold arbitrary solutes and possess unequal sizes. The undisturbed solute concentration gradient is constant over length scales comparable to their center-to-center spacing. The conservative equations for the solute species and fluid momentum applicable to the system are solved by using spherical bipolar coordinates and the fluid streamlines inside and outside the vesicles for various axisymmetric cases are presented. Our numerical results for the vesicle velocities compare favorably with the formulas generated analytically from the method of reflections. It is found that the vesicle interactions in osmophoresis can be significant and peculiar when the vesicles are almost in contact. The two-vesicle interactions are also applied to a theory of concentration effects on transport properties in dilute suspensions to obtain the effect of the vesicle volume fraction on the mean osmophoretic velocity in a bounded dispersion of vesicles.

ANALYSIS FOR THE OSMOPHORESIS OF TWO VESICLES

In this work we consider the osmophoretic motion of two spherical vesicles, each is surrounded by a thin semipermeable membrane, as shown in figure 1. The centers of both vesicles are located on the z -axis. A linear concentration field $C_\infty(x)$ with a uniform solute gradient $E_x e_x + E_z e_z$ (equal to ∇C_∞ , oriented arbitrarily with respect to the line of vesicle centers) is prescribed in the external fluid far away from the pair of vesicles; e_x , e_y and e_z are the unit vectors in the Cartesian coordinate system (x, y, z) . The vesicles may differ in radius, in the average internal concentration of solute and in the hydraulic coefficient of the membrane, but are assumed to maintain their spherical shape. No interaction potential between vesicles is taken into consideration and gravitational effects are ignored. Our purpose is to determine the correction to [3] for one vesicle due to the presence of the other in the concentration and flow fields.

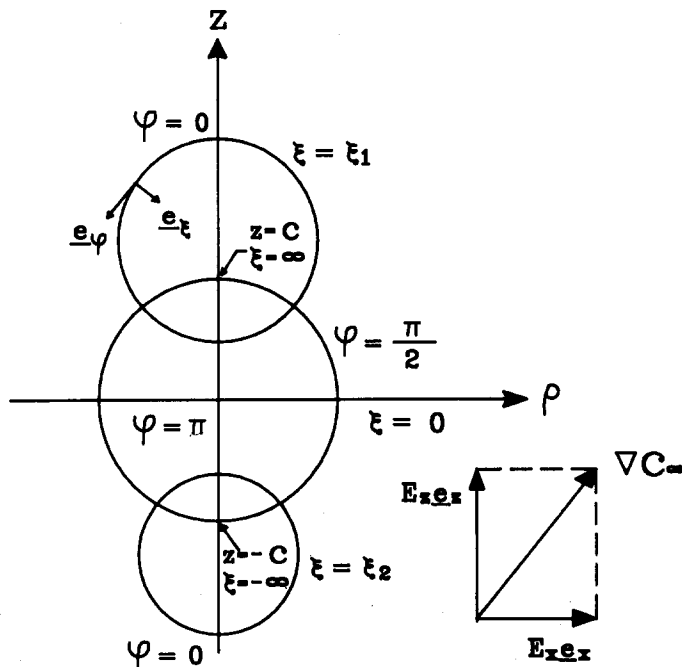


Figure 1. Geometric sketch for the osmophoresis of two spherical vesicles.

To conveniently satisfy the boundary conditions at the vesicle surfaces, the spherical bipolar coordinate system (φ, ξ, ϕ) with the unit vectors \mathbf{e}_φ , \mathbf{e}_ξ and \mathbf{e}_ϕ , illustrated in figure 1, is utilized. This coordinate system is related to the cylindrical polar coordinates (ρ, ϕ, z) by the relation in any meridian plane $\phi = \text{const}$ (Morse & Feshbach 1953; Happel & Brenner 1983):

$$\rho = \frac{c \sin \varphi}{\cosh \xi - \cos \varphi} \quad [5a]$$

and

$$z = \frac{c \sinh \xi}{\cosh \xi - \cos \varphi}, \quad [5b]$$

where $-\infty < \xi < \infty$, $0 \leq \varphi \leq \pi$, and c is a characteristic length which is positive. The coordinate surfaces $\xi = \text{const}$ correspond to a family of non-intersecting coaxial spheres whose centers lie along the z -axis. The special case $\xi = 0$ generates a sphere of infinite radius and represents the plane at $z = 0$. Two spheres external to each other are chosen to be $\xi = \xi_1$ (with $\xi_1 > 0$) and $\xi = \xi_2$ (with $\xi_2 < 0$), and the sphere radii a_1 and a_2 as well as the distances of their centers from the origin d_1 and d_2 are given by

$$a_i = c \operatorname{cosech} |\xi_i| \quad [6a]$$

and

$$d_i = c \coth |\xi_i|, \quad [6b]$$

for $i = 1$ or 2 . The center-to-center distance between the vesicles, r_{12} , equals $d_1 + d_2$.

The interaction between two vesicles in the solute concentration gradient results from three effects: (1) each vesicle disturbs the local solute gradient experienced by the other vesicle; (2) the movement of each vesicle drags surrounding fluid that convects and rotates the other vesicle; (3) each vesicle sucks and ejects fluid causing a reverse flow that affects the motion of the other. To determine the drift velocities of the two vesicles, it is necessary to ascertain the solute concentration and fluid velocity distributions.

Solute concentration distribution

When the migration velocities of the two vesicles are not identical, the transport of momentum and solute species is inherently unsteady. However, the problem can be considered quasisteady if the Peclet and Reynolds numbers are small. The equation of continuity governing the concentration distribution $C(\mathbf{x})$ for the external fluid of constant solute diffusion coefficient D is Laplace's equation:

$$\nabla^2 C = 0. \quad [7a]$$

For the internal fluids of the two vesicles, one has

$$\nabla^2 C_i = 0, \quad i = 1 \text{ or } 2, \quad [7b]$$

where $C_1(\mathbf{x})$ and $C_2(\mathbf{x})$ are the solute concentration fields inside vesicles 1 and 2, respectively.

The radius of each vesicle is much greater than the thickness of its membrane, so that $\xi = \xi_i$ can represent both the inner and the outer membrane surfaces of vesicle i . The boundary conditions require that no solute be transferred across the semipermeable membrane of each vesicle and that the concentration field far away from the vesicles approach the undisturbed value. Thus, for the case of small Peclet number,

$$\xi = \xi_i: \quad \frac{\partial C_i}{\partial \xi} = \frac{c}{\cosh \xi - \mu} \frac{\bar{C}_i}{D_i} (v_{i\xi} - \mathbf{e}_\xi \cdot \mathbf{U}_i) \quad [8a]$$

$$\frac{\partial C}{\partial \xi} = \frac{c}{\cosh \xi - \mu} \frac{C_\infty(\mathbf{x}_i)}{D} (v_{i\xi} - \mathbf{e}_\xi \cdot \mathbf{U}_i); \quad [8b]$$

and

$$(\rho^2 + z^2)^{1/2} \rightarrow \infty: \quad C \rightarrow C_\infty = C_0 + E_x x + E_z z; \quad [8c]$$

for $i = 1$ or 2 ; \bar{C}_1 and \bar{C}_2 are the average internal concentrations of the two vesicles; D_1 and D_2 are the solute diffusion coefficients in the internal fluids; $v_{i\xi}$ and v_ξ together with $v_{i\varphi}$ and v_φ are the velocity components of the internal (inside vesicle i) and external fluids in bispherical coordinates; μ is used to denote $\cos \varphi$ for brevity; $\mathbf{U}_1 (= U_{1x}\mathbf{e}_x + U_{1z}\mathbf{e}_z)$ and $\mathbf{U}_2 (= U_{2x}\mathbf{e}_x + U_{2z}\mathbf{e}_z)$ are the instantaneous osmophoretic velocities of the vesicles to be determined. The undisturbed concentration at the y -axis has been set equal to a constant C_0 for convenience. Thus, the undisturbed concentrations at the vesicle centers are

$$C_\infty(\mathbf{x}_1) = C_0 + E_2 d_1 = C_0 + E_2 c \coth \xi_1 \tag{9a}$$

and

$$C_\infty(\mathbf{x}_2) = C_0 - E_2 d_2 = C_0 + E_2 c \coth \xi_2. \tag{9b}$$

Using [1] and its equilibrium form after the substitution of [2] (Anderson 1983), one can express the fluid velocity at the membrane surface of the vesicle i ($i = 1$ or 2) as

$$\xi = \xi_i: \quad v_\varphi = v_{i\varphi} = \mathbf{e}_\varphi \cdot (\mathbf{U}_i - \boldsymbol{\Omega}_i \times a_i \mathbf{e}_\xi) \tag{10a}$$

$$v_\xi = v_{i\xi} = \mathbf{e}_\xi \cdot \mathbf{U}_i - L_{pi} RT [C - C_\infty(\mathbf{x}_i) - (C_i - \bar{C}_i)]; \tag{10b}$$

where L_{p1} and L_{p2} are the hydraulic coefficients for the membranes of the two vesicles, and $\boldsymbol{\Omega}_1 (= \Omega_1 \mathbf{e}_y)$ and $\boldsymbol{\Omega}_2 (= \Omega_2 \mathbf{e}_y)$ are the instantaneous angular velocities of the vesicles to be determined. To obtain [10b], the Reynolds number and the parameter λ defined by [4c] are assumed to be small. Substitution of [10b] into [8a,b] leads to

$$\xi = \xi_i: \quad \frac{\partial C_i}{\partial \xi} = - \frac{\sinh \xi}{\cosh \xi - \mu} \bar{\kappa}_i [C - C_\infty(\mathbf{x}_i) - (C_i - \bar{C}_i)], \tag{11a}$$

$$\frac{\partial C}{\partial \xi} = - \frac{\sinh \xi}{\cosh \xi - \mu} \kappa_i [C - C_\infty(\mathbf{x}_i) - (C_i - \bar{C}_i)]; \tag{11b}$$

for $i = 1$ or 2 ; the parameters κ_i and $\bar{\kappa}_i$ are defined following [4a,b] by

$$\kappa_i = \frac{a_i L_{pi} R T C_\infty(\mathbf{x}_i)}{D} \tag{12a}$$

and

$$\bar{\kappa}_i = \frac{a_i L_{pi} R T \bar{C}_i}{D_i}. \tag{12b}$$

Thus, the boundary conditions for the concentration field are uncoupled from the vesicle velocities and the flow field.

A general solution to Laplace's equation [7a] suitable for satisfying boundary conditions [11a,b] and [8c] is (Morse & Feshbach 1953; Keh & Chen 1989, 1990):

$$C = cE_x (\cosh \xi - \mu)^{1/2} (1 - \mu)^{1/2} \sum_{n=1}^{\infty} [A_n \cosh(n + \frac{1}{2})\xi + B_n \sinh(n + \frac{1}{2})\xi] P'_n(\mu) \cos \phi + cE_z (\cosh \xi - \mu)^{1/2} \sum_{n=0}^{\infty} [\bar{A}_n \cosh(n + \frac{1}{2})\xi + \bar{B}_n \sinh(n + \frac{1}{2})\xi] P_n(\mu) + C_0 + E_x \rho \cos \phi + E_z z, \tag{13a}$$

where P_n is the Legendre polynomial of order n and the prime means differentiation with respect to μ . Boundary condition [8c] is immediately satisfied by a solution of this form. Because the solute concentration is finite for any position in the interior of each vesicle, the solution to [7b] can be written as

$$C_i = cE_x (\cosh \xi - \mu)^{1/2} (1 - \mu^2)^{1/2} \sum_{n=1}^{\infty} R_{in} \exp[-(n + \frac{1}{2})|\xi|] P'_n(\mu) \cos \phi + cE_z (\cosh \xi - \mu)^{1/2} \times \sum_{n=0}^{\infty} \bar{R}_{in} \exp[-(n + \frac{1}{2})|\xi|] P_n(\mu) + \bar{C}_i + E_x \rho \cos \phi + E_z (z - c \coth \xi_i) \tag{13b}$$

for $i = 1$ or 2 . The coefficients $A_n, B_n, \bar{A}_n, \bar{B}_n, R_{1n}, R_{2n}, \bar{R}_{1n}$ and \bar{R}_{2n} in [13a,b] are to be determined from the boundary conditions at the vesicle surfaces.

Utilizing the expansions, which can be derived using the generating function of the Legendre polynomials,

$$(\cosh \xi - \mu)^{-3/2} = 2\sqrt{2} \sum_{n=1}^{\infty} \exp[-(n + \frac{1}{2})|\xi|] P'_n(\mu) \tag{14a}$$

and

$$\begin{aligned} &(\cosh \xi - \mu)^{-1/2} \cosh \xi - (\cosh \xi - \mu)^{-3/2} \sinh^2 \xi \\ &= \sqrt{2} \sum_{n=0}^{\infty} \exp[-(n + \frac{1}{2})|\xi|] [\cosh \xi - (2n + 1)\sinh|\xi|] P_n(\mu), \end{aligned} \tag{14b}$$

and the recurrence relations of the Legendre polynomials, one can apply [11a,b] to [13a,b] to yield the following formulas for each value of n :

$$\begin{aligned} &(n + 2)\sinh[(n + \frac{3}{2})\xi_i]A_{n+1} + (n + 2)\cosh[(n + \frac{3}{2})\xi_i]B_{n+1} \\ &\quad - [(2n + 1)\cosh \xi_i \sinh(n + \frac{1}{2})\xi_i + \sinh \xi_i \cosh(n + \frac{1}{2})\xi_i]A_n \\ &\quad - [(2n + 1)\cosh \xi_i \cosh(n + \frac{1}{2})\xi_i + \sinh \xi_i \sinh(n + \frac{1}{2})\xi_i]B_n \\ &\quad + (n - 1)\sinh[(n - \frac{1}{2})\xi_i]A_{n-1} + (n - 1)\cosh[(n - \frac{1}{2})\xi_i]B_{n-1} - 2\kappa_i S_{in} \\ &= -4\sqrt{2} \exp[-(n + \frac{1}{2})|\xi_i|] \sinh \xi_i \quad (n \geq 1), \end{aligned} \tag{15a}$$

$$\begin{aligned} &(n + 2)\exp[-(n + \frac{3}{2})|\xi_i|]R_{i(n+1)} - \exp[-(n + \frac{1}{2})|\xi_i|] \\ &\quad \times \left[\sinh \xi_i - \frac{\xi_i}{|\xi_i|} (2n + 1)\cosh \xi_i \right] R_{in} + (n - 1)\exp[-(n - \frac{1}{2})|\xi_i|]R_{i(n-1)} + 2\frac{\xi_i}{|\xi_i|} \bar{\kappa}_i S_{in} \\ &= 4\sqrt{2} \frac{\xi_i}{|\xi_i|} \exp[-(n + \frac{1}{2})|\xi_i|] \sinh \xi_i \quad (n \geq 1), \end{aligned} \tag{15b}$$

$$\begin{aligned} &(n + 1)\sinh[(n + \frac{3}{2})\xi_i]\bar{A}_{n+1} + (n + 1)\cosh[(n + \frac{3}{2})\xi_i]\bar{B}_{n+1} \\ &\quad - [(2n + 1)\cosh \xi_i \sinh(n + \frac{1}{2})\xi_i + \sinh \xi_i \cosh(n + \frac{1}{2})\xi_i]\bar{A}_n \\ &\quad - [(2n + 1)\cosh \xi_i \cosh(n + \frac{1}{2})\xi_i + \sinh \xi_i \sinh(n + \frac{1}{2})\xi_i]\bar{B}_n \\ &\quad + n \sinh[(n - \frac{1}{2})\xi_i]\bar{A}_{n-1} + n \cosh[(n - \frac{1}{2})\xi_i]\bar{B}_{n-1} - 2\frac{\xi_i}{|\xi_i|} \kappa_i \bar{S}_{in} \\ &= 2\sqrt{2} \exp[-(n + \frac{1}{2})|\xi_i|] [\cosh \xi_i - (2n + 1)\sinh|\xi_i|] \quad (n \geq 0) \end{aligned} \tag{15c}$$

and

$$\begin{aligned} &(n + 1)\exp[-(n + \frac{3}{2})|\xi_i|]\bar{R}_{i(n+1)} + \exp[-(n + \frac{1}{2})|\xi_i|] [\sinh|\xi_i| - (2n + 1)\cosh \xi_i] \bar{R}_{in} \\ &\quad + n \exp[-(n - \frac{1}{2})|\xi_i|]\bar{R}_{i(n-1)} + 2\bar{\kappa}_i \bar{S}_{in} \\ &= -2\sqrt{2} \frac{\xi_i}{|\xi_i|} \exp[-(n + \frac{1}{2})|\xi_i|] [\cosh \xi_i - (2n + 1)\sinh|\xi_i|] \quad (n \geq 0), \end{aligned} \tag{15d}$$

where

$$S_{in} = \cosh[(n + \frac{1}{2})\xi_i]A_n + \sinh[(n + \frac{1}{2})\xi_i]B_n - \exp[-(n + \frac{1}{2})|\xi_i|]R_{in}, \tag{16a}$$

$$\bar{S}_{in} = \cosh[(n + \frac{1}{2})\xi_i]\bar{A}_n + \sinh[(n + \frac{1}{2})\xi_i]\bar{B}_n - \exp[-(n + \frac{1}{2})|\xi_i|]\bar{R}_{in} \tag{16b}$$

and $i = 1$ or 2 . Equations [15a,b] represent a group of infinite coupled algebraic equations for the unknown coefficients A_n, B_n, R_{1n} and R_{2n} , and [15c,d] represent a group of similar equations for the unknown coefficients $\bar{A}_n, \bar{B}_n, \bar{R}_{1n}$ and \bar{R}_{2n} . Since these coefficients should individually approach zero as $n \rightarrow \infty$ for the concentration field [13a,b] to remain bounded, they can be determined by

solving the first m sets of the four recurrence relations [15a,b] or [15c,d] with the convention $A_0 = B_0 = R_{10} = R_{20} = 0$ and $\bar{A}_{-1} = \bar{B}_{-1} = \bar{R}_{1(-1)} = \bar{R}_{2(-1)} = 0$, provided that m is sufficiently large that all A_{m+1} , B_{m+1} , $R_{1(m+1)}$, $R_{2(m+1)}$, \bar{A}_m , \bar{B}_m , \bar{R}_{1m} and \bar{R}_{2m} are negligible.

Fluid velocity distribution

Having obtained the solution for the solute concentration field, we can now proceed to find the fluid velocity distribution. Due to the low Reynolds numbers encountered in osmophoretic motions, the Stokes equations apply for the quasisteady fluid motion outside (and also inside) the vesicles:

$$\eta \nabla^2 \mathbf{v} - \nabla p = \mathbf{0} \tag{17a}$$

and

$$\nabla \cdot \mathbf{v} = 0, \tag{17b}$$

where $\mathbf{v}(\mathbf{x})$ is the fluid velocity field for the external flow, and $p(\mathbf{x})$ is the corresponding pressure distribution. The boundary conditions for the velocity field at the membrane surfaces of the two vesicles are given by [10a,b], in which the concentration distributions C and C_i are given by [13a,b] with coefficients determined from [15a–d]. Since the fluid is motionless far away from the vesicles, we have

$$(\rho^2 + z^2)^{1/2} \rightarrow \infty: \mathbf{v} \rightarrow \mathbf{0}. \tag{18}$$

Because the vesicles are freely suspended in the fluid, the net force and net torque exerted by the fluid on the membrane surface of each vesicle must vanish:

$$\mathbf{F}_i = - \iint_{S_i} \mathbf{e}_\zeta \cdot \underline{\underline{\pi}} \, dS_i = \mathbf{0} \tag{19a}$$

and

$$\mathbf{T}_i = \iint_{S_i} a_i \mathbf{e}_\zeta \times (\mathbf{e}_\zeta \cdot \underline{\underline{\pi}}) \, dS_i = \mathbf{0}, \tag{19b}$$

where $\underline{\underline{\pi}}$ is the fluid stress tensor, S_i denotes the surface of vesicle i , and $i = 1$ or 2 . The translational velocities \mathbf{U}_1 and \mathbf{U}_2 as well as the angular velocities $\boldsymbol{\Omega}_1$ and $\boldsymbol{\Omega}_2$ can be evaluated by satisfying constraints [19a,b] after solving [17a,b], [10a,b] and [18]. Using the divergence theorem to convert the surface integrals in [19a,b] to volume integrals and applying the fact that

$$\nabla \cdot \underline{\underline{\pi}} = \mathbf{0} \tag{20}$$

and the symmetry of $\underline{\underline{\pi}}$ in Stoke's flow, one can show that the fluid inside a vesicle always acts no net force and torque on the inner surface of the vesicle. Thus, only the forces and torques exerted by the external fluid on the vesicles are to be considered to determine the vesicle velocities.

Since the governing equations and boundary conditions concerning the problem of osmophoresis of two vesicles oriented at an arbitrary angle to the undisturbed solute gradient ($E_x \mathbf{e}_x + E_z \mathbf{e}_z$) are linear, it is possible to decompose the problem into two subproblems: motion due to a solute gradient perpendicular to the line between vesicle centers ($E_z = 0$) and motion due to a solute gradient parallel to the line ($E_x = 0$). The net solution for the general problem can be obtained by adding the solutions from both subproblems vectorially.

First, we consider the osmophoretic motion of two vesicles perpendicular to their line of centers. For this case, $\mathbf{U}_i = U_{ix} \mathbf{e}_x$ for $i = 1$ and 2 . A general solution of [17a] satisfying the boundary condition [18] is (Dean & O'Neill 1963; O'Neill 1964):

$$v_\rho = \frac{1}{2c} [\rho Q_1 + c(V_2 + V_0)] \cos \phi, \tag{21a}$$

$$v_z = \frac{1}{2c} [z Q_1 + 2c W_1] \cos \phi, \tag{21b}$$

$$v_\phi = \frac{1}{2} (V_2 - V_0) \sin \phi \tag{21c}$$

and

$$p = \frac{1}{c} \eta Q_1 \cos \phi. \quad [21d]$$

In the above equations, Q_1 , V_0 , V_2 and W_1 are scalar auxiliary functions of ρ and z (or of ξ and ϕ), with the following expansion forms:

$$W_1 = (\cosh \xi - \mu)^{1/2} (1 - \mu^2)^{1/2} \sum_{n=1}^{\infty} [a_n \cosh(n + \frac{1}{2})\xi + b_n \sinh(n + \frac{1}{2})\xi] P'_n(\mu), \quad [22a]$$

$$Q_1 = (\cosh \xi - \mu)^{1/2} (1 - \mu^2)^{1/2} \sum_{n=1}^{\infty} [c_n \cosh(n + \frac{1}{2})\xi + d_n \sinh(n + \frac{1}{2})\xi] P'_n(\mu), \quad [22b]$$

$$V_0 = (\cosh \xi - \mu)^{1/2} \sum_{n=0}^{\infty} [e_n \cosh(n + \frac{1}{2})\xi + f_n \sinh(n + \frac{1}{2})\xi] P_n(\mu) \quad [22c]$$

and

$$V_2 = (\cosh \xi - \mu)^{1/2} (1 - \mu^2) \sum_{n=2}^{\infty} [g_n \cosh(n + \frac{1}{2})\xi + h_n \sinh(n + \frac{1}{2})\xi] P''_n(\mu). \quad [22d].$$

The coefficients a_n , b_n , c_n , d_n , e_n , f_n , g_n and h_n remain to be determined from the equation of continuity [17b] and the boundary conditions [10a,b].

Substituting the solution for the solute concentration distributions, [13a,b], with $E_z = 0$ and coefficients determined by [15a,b], as well as the expression for the fluid velocity, [21a-d] and [22a-d], into the boundary conditions [10a,b], it is found that the coefficients of the auxiliary functions must satisfy 6 algebraic recurrence formulas for each value of $n \geq 0$. These formulas are lengthy, so we list them in table 1. The recurrence relations of the Legendre polynomials and expansions derived from generating function of the Legendre polynomials were used to expand the boundary conditions.

Table 1. Recursion formulas for the evaluation of the coefficients in [22a-d] (all formulas are valid for $i = 1$ or 2)

$$\begin{aligned} c_n \cosh(n + \frac{1}{2})\xi_i + d_n \sinh(n + \frac{1}{2})\xi_i &= \frac{-2}{\sinh \xi_i} \left[\frac{-n-2}{2n+3} H_{n+1} + \cosh \xi_i H_n + \frac{-n+1}{2n-1} H_{n-1} \right] \\ &\quad - \sqrt{8c\Omega} \operatorname{cosech} \xi_i \left\{ \frac{1}{2n-1} \exp[-(n-\frac{1}{2})|\xi_i|] - \frac{1}{2n+3} \exp[-(n+\frac{3}{2})|\xi_i|] \right\} \\ &\quad - 2 \frac{\xi_i}{|\xi_i|} L_{pi} RTE_x c \operatorname{cosech} \xi_i \left[\frac{-n-2}{2n+3} \cosh \xi_i S_{n+1} + S_n + \frac{-n+1}{2n-1} \cosh \xi_i S_{n-1} \right] \\ e_n \cosh(n + \frac{1}{2})\xi_i + f_n \sinh(n + \frac{1}{2})\xi_i &= \operatorname{cosech} \xi_i \left[\frac{(n+1)(n+2)}{2n+3} H_{n+1} - \frac{(n-1)n}{2n-1} H_{n-1} \right] \\ &\quad + \sqrt{8} \frac{\xi_i}{|\xi_i|} c\Omega (2n+1) \exp[-(n+\frac{1}{2})|\xi_i|] - \sqrt{8} \left[\frac{\xi_i}{|\xi_i|} \Omega D_i - U_{ix} \right] \exp[-(n+\frac{1}{2})|\xi_i|] \\ &\quad + \sqrt{8c\Omega} \operatorname{cosech} \xi_i \left\{ \frac{(n+1)(n+2)}{2n+3} \exp[-(n+\frac{3}{2})|\xi_i|] - \frac{n(n-1)}{2n-1} \exp[-(n-\frac{1}{2})|\xi_i|] \right\} \\ &\quad + \frac{\xi_i}{|\xi_i|} L_{pi} RTE_x c \coth \xi_i \left[\frac{(n+1)(n+2)}{2n+3} S_{n+1} - \frac{(n-1)n}{2n-1} S_{n-1} \right] \\ g_n \cosh(n + \frac{1}{2})\xi_i + h_n \sinh(n + \frac{1}{2})\xi_i &= \operatorname{cosech} \xi_i \left[\frac{1}{2n-1} H_{n-1} - \frac{1}{2n+3} H_{n+1} \right] \\ &\quad + \sqrt{8c\Omega} \operatorname{cosech} \xi_i \left\{ \frac{1}{2n-1} \exp[-(n-\frac{1}{2})|\xi_i|] - \frac{1}{2n+3} \exp[-(n+\frac{3}{2})|\xi_i|] \right\} \\ &\quad + \frac{\xi_i}{|\xi_i|} L_{pi} RTE_x c \coth \xi_i \left[\frac{1}{2n-1} S_{n-1} - \frac{1}{2n+3} S_{n+1} \right] \end{aligned}$$

In this table, $H_n = a_n \cosh(n + \frac{1}{2})\xi_i + b_n \sinh(n + \frac{1}{2})\xi_i$ and S_n is defined by [16a].

We have, up to now, 8 sets of unknowns but only 6 sets of equations. However, the equation of continuity has not yet been satisfied. By substituting [21a-d] and [22a-d] into [17b], two more relations among the coefficients result (Dean & O'Neill 1963; O'Neill 1964):

$$(n + 2)c_{n+1} + 5c_n - (n - 1)c_{n-1} - e_{n+1} + 2e_n - e_{n-1} + (n + 2)(n + 3)g_{n+1} - 2(n - 1)(n + 2)g_n + (n - 2)(n - 1)g_{n-1} - 2(n + 2)b_{n+1} + 2(2n + 1)b_n - 2(n - 1)b_{n-1} = 0 \quad [23a]$$

and

$$(n + 2)d_{n+1} + 5d_n - (n - 1)d_{n-1} - f_{n+1} + 2f_n - f_{n-1} + (n + 2)(n + 3)h_{n+1} - 2(n - 1)(n + 2)h_n + (n - 2)(n - 1)h_{n-1} - 2(n + 2)a_{n+1} + 2(2n + 1)a_n - 2(n - 1)a_{n-1} = 0. \quad [23b]$$

Because the unknown coefficients a_n, b_n, \dots and h_n become small with large n , simultaneous solution of the 6 equations in table 1 and [23a,b] for the first m sets yields $8m$ coefficients in terms of the unknown vesicle velocities U_{1x}, U_{2x}, Ω_1 and Ω_2 , thereby determining the velocity and pressure distributions for the external fluid according to [21a-d] and [22a-d].

The drag force on the surface of the vesicle at $\xi = \xi_1$ and the torque on the surface about the vesicle center exerted by the external fluid can be expressed as (Wakiya 1967):

$$\mathbf{F}_1 = -2\sqrt{2}\pi\eta c \sum_{n=0}^{\infty} (e_n + f_n)\mathbf{e}_x \quad [24a]$$

and

$$\mathbf{T}_1 = -2\sqrt{2}\pi\eta c^2 \sum_{n=0}^{\infty} (2n + 1 - \coth \xi_1)(e_n + f_n)\mathbf{e}_y. \quad [24b]$$

The corresponding results for the vesicle at $\xi = \xi_2$ are

$$\mathbf{F}_2 = 2\sqrt{2}\pi\eta c \sum_{n=0}^{\infty} (e_n - f_n)\mathbf{e}_x \quad [24c]$$

and

$$\mathbf{T}_2 = 2\sqrt{2}\pi\eta c^2 \sum_{n=0}^{\infty} (2n + 1 + \coth \xi_2)(e_n - f_n)\mathbf{e}_y. \quad [24d]$$

Since the fluid inside a vesicle exerts no net force and torque on the inner surface of the vesicle, the above formulas also represent the net forces and net torques exerted by both the external and internal fluids on the vesicles. The vesicle velocities U_{1x}, U_{2x}, Ω_1 and Ω_2 can be obtained by solving the four equations in the second part of [19a,b] incorporated with [24a-d].

We now consider the osmophoresis of two vesicles along their line of centers. For this axisymmetric case, $\mathbf{U}_i = U_{iz}\mathbf{e}_z$ and $\Omega_i = 0$ for $i = 1$ and 2 . Also, the fluid velocities inside and outside the vesicles are governed by the quasisteady fourth-order differential equations,

$$E^4\Psi = E^2(E^2\Psi) = 0 \quad [25a]$$

$$E^4\Psi_i = 0, \quad i = 1 \text{ or } 2, \quad [25b]$$

where Ψ_i and Ψ are the Stokes stream functions for the flow inside vesicle i and for the external flow, respectively. The operator E^2 assumes the following form in bispherical coordinates:

$$E^2 = \frac{\cosh \xi - \mu}{c^2} \left\{ \frac{\partial}{\partial \xi} \left[(\cosh \xi - \mu) \frac{\partial}{\partial \xi} \right] + (1 - \mu^2) \frac{\partial}{\partial \mu} \left[(\cosh \xi - \mu) \frac{\partial}{\partial \mu} \right] \right\}. \quad [26]$$

The stream function Ψ (or Ψ_i) is related to the velocity field \mathbf{v} (or \mathbf{v}_i) by the formulas

$$v_\xi = -\frac{(\cosh \xi - \mu)^2}{c^2} \frac{\partial \Psi}{\partial \mu} \quad [27a]$$

and

$$v_\varphi = -\frac{(\cosh \xi - \mu)^2}{c^2(1 - \mu)^{1/2}} \frac{\partial \Psi}{\partial \xi}. \quad [27b]$$

General solutions of [25a,b] satisfying the boundary condition [18] and the requirement of finite velocity in the interior of each vesicle are (Stimson & Jeffery 1926; Haber *et al.* 1973):

$$\Psi = c^2(\cosh \xi - \mu)^{-3/2} \sum_{n=1}^{\infty} \{ \bar{a}_n \cosh[(n - \frac{1}{2})\xi] + \bar{b}_n \sinh[(n - \frac{1}{2})\xi] + \bar{c}_n \cosh[(n + \frac{3}{2})\xi] + \bar{d}_n \sinh[(n + \frac{3}{2})\xi] \} G_{n+1}^{-1/2}(\mu) \tag{28a}$$

and

$$\Psi_i = c^2(\cosh \xi - \mu)^{-3/2} \sum_{n=1}^{\infty} \{ \bar{e}_{in} \exp[-(n - \frac{1}{2})|\xi|] + \bar{f}_{in} \exp[-(n + \frac{3}{2})|\xi|] \} G_{n+1}^{-1/2}(\mu), \tag{28b}$$

for $i = 1$ or 2 . $G_{n+1}^{-1/2}(\mu)$ is the Gegenbauer polynomial of order $n + 1$ and degree $-1/2$, which is related to the Legendre polynomials via the relation

$$G_{n+1}^{-1/2}(\mu) = \frac{P_{n-1}(\mu) - P_{n+1}(\mu)}{2n + 1}. \tag{29}$$

The coefficients $\bar{a}_n, \bar{b}_n, \bar{c}_n, \bar{d}_n, \bar{e}_{in}$ and \bar{f}_{in} in [28a,b] are to be determined from the boundary conditions [10a,b] using [14b] and the recurrence relations of the Legendre and Gegenbauer polynomials. The procedure is straightforward but tedious, and the results which consist of 8 algebraic recurrence formulas (4 for $\bar{a}_n, \bar{b}_n, \bar{c}_n$ and \bar{d}_n ; 2 for \bar{e}_{1n} and \bar{f}_{1n} ; and 2 for \bar{e}_{2n} and \bar{f}_{2n}) for each value of $n \geq 1$ are given in table 2. Since the unknown coefficients $\bar{a}_n, \bar{b}_n, \dots$ and \bar{f}_{2n} become small with a large n , simultaneous solution of 8 recursion equations in table 2 for the first m sets yields $8m$ coefficients in terms of the unknown vesicle velocities U_{1z} and U_{2z} , thereby determining the Stokes stream functions for the fluid according to [28a,b].

Table 2. Recursion formulas for the evaluation of the coefficients in [28a,b] (all formulas are valid for $i = 1$ or 2)

$\frac{-2n-5}{2(2n+3)} [\bar{a}_{n+1} \cosh(n + \frac{1}{2})\xi_i + \bar{b}_{n+1} \sinh(n + \frac{1}{2})\xi_i + \bar{c}_{n+1} \cosh(n + \frac{5}{2})\xi_i + \bar{d}_{n+1} \sinh(n + \frac{5}{2})\xi_i]$ $= -\cosh \xi_i [\bar{a}_n \cosh(n - \frac{1}{2})\xi_i + \bar{b}_n \sinh(n - \frac{1}{2})\xi_i + \bar{c}_n \cosh(n + \frac{3}{2})\xi_i + \bar{d}_n \sinh(n + \frac{3}{2})\xi_i]$ $- \frac{-2n+3}{2(2n-1)} [\bar{a}_{n-1} \cosh(n - \frac{3}{2})\xi_i + \bar{b}_{n-1} \sinh(n - \frac{3}{2})\xi_i + \bar{c}_{n-1} \cosh(n + \frac{1}{2})\xi_i + \bar{d}_{n-1} \sinh(n + \frac{1}{2})\xi_i]$ $- L_{pi} RTE_i c \frac{\xi_i}{ \xi_i } \left[\frac{-n}{2n-1} \bar{S}_{(n-1)} + \cosh \xi_i \bar{S}_n + \frac{-n-1}{2n+3} \bar{S}_{(n+1)} \right]$ $+ U_{iz} \sqrt{2} \left\{ \frac{-n}{2n-1} \cosh \xi_i \exp[-(n - \frac{1}{2}) \xi_i] + \exp[-(n + \frac{1}{2}) \xi_i] + \frac{-n-1}{2n+3} \cosh \xi_i \exp[-(n + \frac{3}{2}) \xi_i] \right\}$
$\frac{n(2n+1)}{2n+3} [\bar{a}_{n+1} \sinh(n + \frac{1}{2})\xi_i + \bar{b}_{n+1} \cosh(n + \frac{1}{2})\xi_i] + \frac{n(2n+5)}{2n+3} [\bar{c}_{n+1} \sinh(n + \frac{5}{2})\xi_i + \bar{d}_{n+1} \cosh(n + \frac{5}{2})\xi_i]$ $= -3 \sinh \xi_i [\bar{a}_n \cosh(n - \frac{1}{2})\xi_i + \bar{b}_n \sinh(n - \frac{1}{2})\xi_i + \bar{c}_n \cosh(n + \frac{3}{2})\xi_i + \bar{d}_n \sinh(n + \frac{3}{2})\xi_i]$ $+ \cosh \xi_i \{ (2n-1) [\bar{a}_n \sinh(n - \frac{1}{2})\xi_i + \bar{b}_n \cosh(n - \frac{1}{2})\xi_i] + (2n+3) [\bar{c}_n \sinh(n + \frac{3}{2})\xi_i + \bar{d}_n \cosh(n + \frac{3}{2})\xi_i] \}$ $- (n+1) \left\{ \frac{2n-3}{2n-1} [\bar{a}_{n-1} \sinh(n - \frac{3}{2})\xi_i + \bar{b}_{n-1} \cosh(n - \frac{3}{2})\xi_i] + \frac{2n+1}{2n-1} [\bar{c}_{n-1} \sinh(n + \frac{1}{2})\xi_i + \bar{d}_{n-1} \cosh(n + \frac{1}{2})\xi_i] \right\}$ $- U_{iz} 2\sqrt{2} \sinh \xi_i \left\{ \frac{n(n+1)}{2n-1} \exp[-(n - \frac{1}{2}) \xi_i] - \frac{n(n+1)}{2n+3} \exp[-(n + \frac{3}{2}) \xi_i] \right\}$
$\bar{e}_{in} \exp[-(n - \frac{1}{2}) \xi_i] + \bar{f}_{in} \exp[-(n + \frac{3}{2}) \xi_i] = \bar{a}_n \cosh[(n - \frac{1}{2})\xi_i] + \bar{b}_n \sinh[(n - \frac{1}{2})\xi_i] + \bar{c}_n \cosh[(n + \frac{3}{2})\xi_i] + \bar{d}_n \sinh[(n + \frac{3}{2})\xi_i]$
$\frac{\xi_i}{ \xi_i } \{ \bar{e}_{in} (2n-1) \exp[-(n - \frac{1}{2}) \xi_i] + \bar{f}_{in} (2n+3) \exp[-(n + \frac{3}{2}) \xi_i] \}$ $= -(2n-1) \{ \bar{a}_n \sinh[(n - \frac{1}{2})\xi_i] + \bar{b}_n \cosh[(n - \frac{1}{2})\xi_i] \}$ $- (2n+3) \{ \bar{c}_n \sinh[(n + \frac{3}{2})\xi_i] + \bar{d}_n \cosh[(n + \frac{3}{2})\xi_i] \}$

By integration of the total stress on the membrane surface of each vesicle, the drag force opposing the axisymmetric osmophoretic motion of the vesicle at $\xi = \xi_1$ is (Stimson & Jeffery 1926; Happel & Brenner 1983):

$$\mathbf{F}_1 = -2\sqrt{2}\pi\eta c \sum_{n=1}^{\infty} (\bar{a}_n + \bar{b}_n + \bar{c}_n + \bar{d}_n)\mathbf{e}_z; \tag{30a}$$

and for the vesicle at $\xi = \xi_2$,

$$\mathbf{F}_2 = -2\sqrt{2}\pi\eta c \sum_{n=1}^{\infty} (\bar{a}_n - \bar{b}_n + \bar{c}_n - \bar{d}_n)\mathbf{e}_z. \tag{30b}$$

Note that the fluid inside a vesicle exerts no net force on the inner surface of the vesicle. To determine the instantaneous osmophoretic velocities U_{1z} and U_{2z} of the vesicles, the two equations in the second part of [19a] incorporated with [30a,b] must be solved.

Mobility parameters of vesicles

Owing to the linearity of the governing equations [7a,b] and [17a,b] as well as the boundary conditions [11a,b], [10a,b] and [18], the results of osmophoretic velocities for the general problem of two spherical vesicles oriented arbitrarily relative to the undisturbed solute gradient can be expressed as (for $i = 1$ or 2):

$$\mathbf{U}_i = \sum_{j=1}^2 [M_{ij}^{(p)}\mathbf{e}\mathbf{e} + M_{ij}^{(n)}(\mathbf{I} - \mathbf{e}\mathbf{e})] \cdot \mathbf{U}_j^{(0)} \tag{31a}$$

and

$$a_i\boldsymbol{\Omega}_i = -\sum_{j=1}^2 N_{ij}\mathbf{e} \times \mathbf{U}_j^{(0)}, \tag{31b}$$

where

$$\mathbf{U}_j^{(0)} = -\frac{1}{2}a_jL_{pj}RT[1 + \bar{\kappa}_j + \frac{1}{2}\kappa_j]^{-1}\nabla C_{\infty}, \tag{32}$$

which is the osmophoretic velocity of the vesicle j in the absence of the other and is computed from [3] taking $\lambda = 0$. In [31a,b], \mathbf{e} is the unit vector directed from the center of vesicle 1 toward the center of vesicle 2 and \mathbf{I} is the unit dyadic. The dimensionless mobility parameters $M_{ij}^{(p)}$, $M_{ij}^{(n)}$ and N_{ij} are functions of the relative sizes and separation distance of the vesicles as well as the system properties. Obviously, when the two vesicles are separated by an infinite distance, we have

$$M_{ii}^{(p)} = M_{ii}^{(n)} = 1, \tag{33a}$$

$$M_{ij}^{(p)} = M_{ij}^{(n)} = 0 \quad (j = 1, 2, \text{ but } j \neq i) \tag{33b}$$

and

$$N_{ij} = 0 \quad (j = 1, 2), \tag{33c}$$

for $i = 1$ or 2 .

The numerical solution of $M_{11}^{(p)}$, $M_{12}^{(p)}$, $M_{21}^{(p)}$ and $M_{22}^{(p)}$ can be obtained by solving the problem of osmophoretic motion of two vesicles along their line of centers, while the solution of the remaining 8 parameters ($M_{ij}^{(n)}$ and N_{ij}) can be obtained by solving the problem of osmophoresis of two vesicles perpendicular to the line between centers. The detailed results will be presented in the next section.

RESULTS AND DISCUSSION

Using a 32-bit personal computer, the coefficients of the solute concentration distributions [13a,b], of the auxiliary functions for the velocity field [22a–d] and of the fluid stream functions [28a,b] in the present quasisteady problem have been calculated for various values of κ_1 , κ_2 , $\bar{\kappa}_1$, $\bar{\kappa}_2$, a_2/a_1 and $(a_1 + a_2)/r_{12}$. For the difficult case of a large size ratio ($a_2/a_1 = 5.0$) and small gap thickness [$(a_1 + a_2)/r_{12} = 0.995$], $m = 510$ is sufficiently large that the $(m + 1)$ th terms of these

coefficients are negligible and an increase in m does not alter the calculated values appreciably. In the following we present the results of the fluid streamlines for the axisymmetric cases and of the vesicles' velocities for the general situations. Also, the interaction effects between pairs of vesicles will be extended to the calculation of the average osmophoretic velocity of small vesicles in a statistically homogeneous dispersion.

Streamlines

The streamline pattern for the fluid inside and outside a single osmophoretic vesicle was exhibited graphically by Anderson (1983, 1986). The distortion of the fluid flow due to interactions between two vesicles undergoing osmophoresis along their line of centers is illustrated in figures 2 and 3.

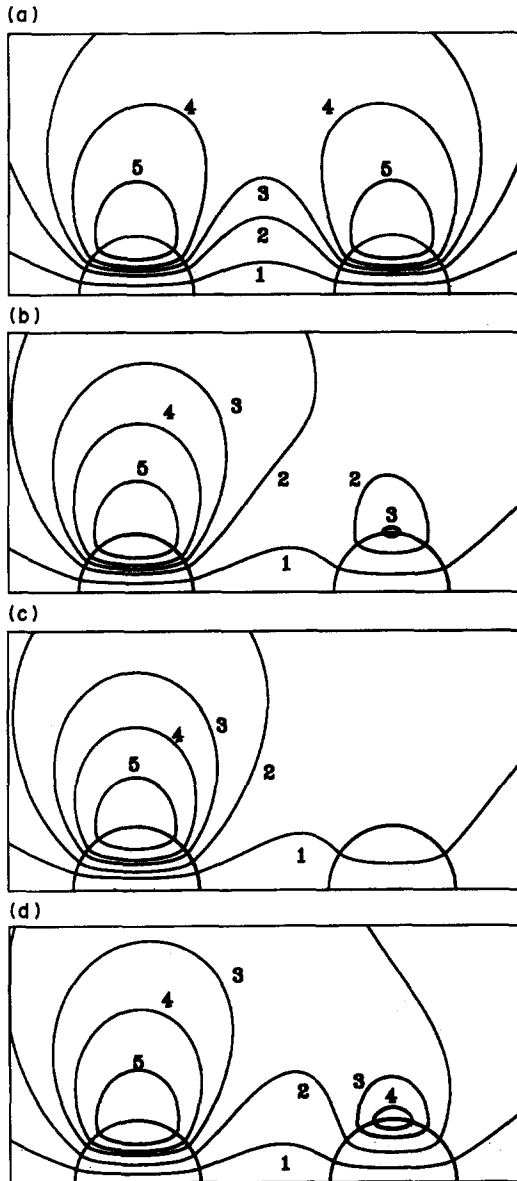


Figure 2. Streamlines for the axisymmetric osmophoretic motion of two spherical vesicles of identical radii and hydraulic coefficients with $2a/r_{12} = 0.5$. The left hemisphere represents vesicle 1. (a) $\kappa_1 = \kappa_2 = \bar{\kappa}_1 = \bar{\kappa}_2 = 0$; (b) $\kappa_1 = \bar{\kappa}_1 = \bar{\kappa}_2 = 0$; $\kappa_2 = 5$; (c) $\kappa_1 = \kappa_2 = \bar{\kappa}_1 = 0$, $\bar{\kappa}_2 = 5$; (d) $\bar{\kappa}_1 = 0$, $\kappa_1 = \kappa_2 = \bar{\kappa}_2 = 5$. $\Psi/c^2U_1^{(0)}$: 1, 0.05; 2, 0.2; 3, 0.3; 4, 0.4; 5, 0.6.

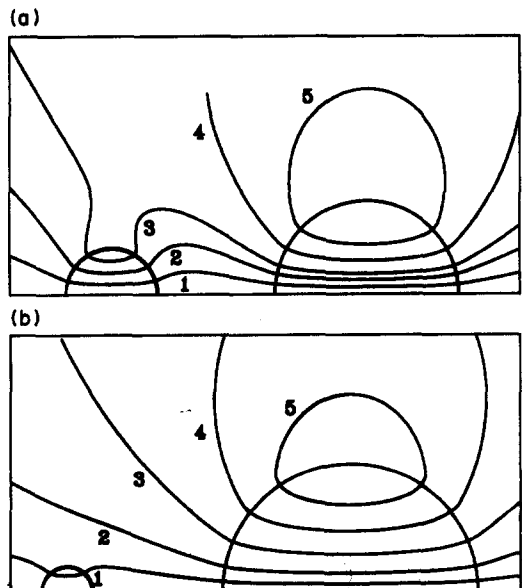


Figure 3. Streamlines for the axisymmetric osmophoretic motion of two spherical vesicles of unequal radii with $(a_1 + a_2)/r_{12} = 0.6$, $L_{p1} = L_{p2}$ and $\kappa_1 = \kappa_2 = \bar{\kappa}_1 = \bar{\kappa}_2 = 0$. (a) $a_2/a_1 = 2.0$, $\Psi/c^2U_1^{(0)}$: 1, 0.1; 2, 0.4; 3, 0.8; 4, 2.0; 5, 4.0. (b) $a_2/a_1 = 5.0$, $\Psi/c^2U_1^{(0)}$: 1, 0.5; 2, 2.0; 3, 10; 4, 30; 5, 60.

In each case, streamlines in a meridian plane are depicted. Figures 2(a-d) picture the situation when the two spheres have identical radii and hydraulic coefficients and the distance between the vesicle surfaces is equal to the sum of their radii. The contour pattern in figure 2(a) corresponding to the case of $\kappa_1 = \kappa_2 = \bar{\kappa}_1 = \bar{\kappa}_2 = 0$ (small hydraulic coefficients, and/or small solute concentrations and/or large solute diffusivities) shows equivalent local recirculations in the vicinity of each sphere and a symmetric global recirculation pattern far away from the vesicles. For two identical vesicles ($\kappa_1 = \kappa_2 = \kappa$, $\bar{\kappa}_1 = \bar{\kappa}_2 = \bar{\kappa}$ and $a_1 = a_2 = a$) with finite values of κ and/or $\bar{\kappa}$, the streamlines will show a similar flow pattern. These balanced recirculations will be distorted if the two vesicles differ in the values of κ or $\bar{\kappa}$, as shown in figures 2(b-d). It can be seen that the spacing between streamlines in the vesicle with the smaller value of κ or $\bar{\kappa}$ is narrower and the local fluid recirculation is stronger than that for the other vesicle, which shows a larger migration velocity for the former vesicle. These results are consistent with the prediction of [3].

The situation of two spheres with $L_{p1} = L_{p2}$ and $\kappa_1 = \kappa_2 = \bar{\kappa}_1 = \bar{\kappa}_2 = 0$ but unequal radii is depicted in figures 3(a) and (b), which correspond to the cases of $a_2/a_1 = 2.0$ and $a_2/a_1 = 5.0$, respectively, with $(a_1 + a_2)/r_{12} = 0.6$. Again, as expected from [3], the larger vesicle migrates faster. It is noted that the local recirculation in the vicinity of the larger vesicle is substantial, whereas it might disappear in the vicinity of the smaller vesicle. As the radius ratio becomes large, the fluid flow is dominated by the larger vesicle, with the smaller one introducing only local perturbations. Note that the corresponding patterns of the solute concentration distribution (curves of constant concentration) in the external fluid to figures 2(a) and 3 ($\kappa_1 = \kappa_2 = \bar{\kappa}_1 = \bar{\kappa}_2 = 0$) are exactly the same as those for the temperature distribution (isotherms) in the case of

Table 3. The mobility parameters $M_{ij}^{(p)}$, $M_{ij}^{(n)}$ and N_{ij} ($i, j = 1$ or 2), defined by [31a,b], for the osmophoretic motion of two identical vesicles ($L_{p1} = L_{p2}$, $a_1 = a_2 = a$, $\kappa_1 = \kappa_2 = \kappa$, $\bar{\kappa}_1 = \bar{\kappa}_2 = \bar{\kappa}$) with $\kappa = \bar{\kappa} = 0$; the results of the asymptotic solution are evaluated from [34a,b] as a comparison

$\frac{2a}{r_{12}}$	$M_{11}^{(p)} = M_{22}^{(p)}$	$M_{12}^{(p)} = M_{21}^{(p)}$			$M_{11}^{(n)} + M_{12}^{(n)}$	
			Exact solution	Asymptotic solution	Exact solution	Asymptotic solution
0.1	0.999875	-0.000250	0.999625	0.999625	0.999625	0.999625
0.2	0.999016	-0.001993	0.997023	0.997023	0.997023	0.997023
0.3	0.996810	-0.006673	0.990137	0.990137	0.990137	0.990137
0.4	0.993056	-0.015585	0.977471	0.977471	0.977471	0.977471
0.5	0.988441	-0.029823	0.958618	0.958618	0.958618	0.958618
0.6	0.985262	-0.050541	0.934721	0.934721	0.935767	0.935767
0.7	0.988628	-0.080281	0.908347	0.908347	0.913655	0.913655
0.8	1.009954	-0.127541	0.882413	0.882413	0.902208	0.902208
0.9	1.084530	-0.225739	0.858791	0.858791	0.917612	0.917612
0.95	1.185854	-0.337804	0.848050	0.848050	0.942658	0.942658
0.97	1.261685	-0.417729	0.843956	0.843956	0.957097	0.957097
0.98	1.316199	-0.474250	0.841949	0.841949	0.965403	0.965403
0.99	1.391666	-0.551697	0.839969	0.839969	0.974482	0.974482
0.995	1.44403	-0.60504	0.83899	0.83899	0.979325	0.979325

$\frac{2a}{r_{12}}$	$M_{11}^{(n)} = M_{22}^{(n)}$	$M_{12}^{(n)} = M_{21}^{(n)}$	$N_{11} = -N_{22}$	$N_{12} = -N_{21}$	$M_{11}^{(n)} + M_{12}^{(n)}$		$M_{11}^{(n)} + M_{12}^{(n)}$
					Exact solution	Asymptotic solution	
0.1	1.000063	0.000125	0.571E-8	0.197E-8	1.000188	0.768E-8	1.000188
0.2	1.000500	0.001001	0.776E-6	0.259E-6	1.001501	0.104E-5	1.001501
0.3	1.001690	0.003381	0.139E-4	0.467E-5	1.005071	0.186E-4	1.005071
0.4	1.004009	0.008031	0.000112	0.383E-4	1.012040	0.000150	1.012048
0.5	1.007826	0.015739	0.000590	0.000209	1.023565	0.000799	1.023621
0.6	1.013422	0.027324	0.002409	0.000915	1.040746	0.003324	1.041047
0.7	1.020700	0.043613	0.008466	0.003567	1.064313	0.012033	1.065691
0.8	1.028007	0.065245	0.027878	0.013483	1.093252	0.041361	1.099072
0.9	1.025948	0.090861	0.09827	0.05647	1.116809	0.15474	1.142915
0.95	1.004508	0.099360	0.21591	0.13844	1.103868	0.35435	1.169372
0.97	0.978643	0.095728	0.32923	0.22351	1.074371	0.55274	1.180888
0.98	0.953421	0.087716	0.43318	0.30516	1.041137	0.73834	1.186854
0.99	0.90280	0.06491	0.63695	0.47199	0.96772	1.10884	1.192964
0.995	0.8445	0.0318	0.8716	0.6733	0.8763	1.5449	1.196073

thermocapillary motion of two gas bubbles in a thermal gradient, which were depicted by Meyyappan *et al.* (1983).

Vesicle velocities

The numerical results of the mobility parameters $M_{ij}^{(p)}$, $M_{ij}^{(n)}$ and N_{ij} ($i, j = 1$ or 2), defined by [31a,b], for the case of two identical vesicles with various values of κ , $\bar{\kappa}$ and $2a/r_{12}$ are presented in tables 3 and 4. These values are convergent at least to the digits as shown. The two identical vesicles will translate at the same velocity because $M_{11}^{(p,n)} = M_{22}^{(p,n)}$, $M_{22}^{(p,n)} = M_{11}^{(p,n)}$ and $U_2^{(0)} = U_1^{(0)}$. For the osmophoresis of two vesicles along their line of centers, the results in tables 3 and 4 demonstrate that the interaction between vesicles decreases rapidly, for all values of κ and $\bar{\kappa}$, with an increase in the gap between them (i.e. decreasing $2a/r_{12}$). However, the vesicles' interaction can be strong when the surface-to-surface spacing gets close to zero. Note that, because the reverse fluid motion against the migration of one vesicle convects the other, the two identical vesicles move slower than either would move in the absence of the other. This particular behavior for osmophoresis is opposite to that for the axisymmetric sedimentation (Haber *et al.* 1973) or thermocapillary migration (Keh & Chen 1990) of two fluid droplets.

It can be found from tables 3 and 4 that the translational velocity of the two identical vesicles undergoing osmophoresis normal to their line of centers is a monotonic increasing function of the separation parameter $2a/r_{12}$ for all $2a/r_{12} \lesssim 0.9$. This effect, which is due to the fact that the fluid recirculation generated by the movement of one vesicle convects the other, is opposite to the behavior of the osmophoretic motion of two identical vesicles along their line of centers. On the other hand, as $2a/r_{12} \gtrsim 0.9$, the vesicle velocity decreases with increasing $2a/r_{12}$ and can even be smaller than the value the vesicles would possess if isolated when they are almost in contact. Under this situation, the strong fluid recirculation in the vicinity of one vesicle can hinder the other from sucking or ejecting solvent through its membrane. Note that the two identical vesicles rotate about an axis perpendicular to both \mathbf{e} and ∇C_∞ with the same magnitude, which increases monotonically

Table 4. The mobility parameters $M_{ij}^{(p)}$, $M_{ij}^{(n)}$ and N_{ij} ($i, j = 1$ or 2) for the osmophoretic motion of two identical vesicles with various values of κ , $\bar{\kappa}$ and $2a/r_{12}$

κ	$\bar{\kappa}$	$\frac{2a}{r_{12}}$	$M_{11}^{(p)} = M_{22}^{(p)}$	$M_{12}^{(p)} = M_{21}^{(p)}$	$M_{11}^{(n)} = M_{22}^{(n)}$	$M_{12}^{(n)} = M_{21}^{(n)}$	$N_{11} = -N_{22}$	$N_{12} = -N_{21}$		
0	5	0.2	0.99736	-0.00033	1.00133	0.00017	0.11E-5	0.13E-6		
		0.4	0.98019	-0.00248	1.01061	0.00133	0.00016	0.19E-4		
		0.6	0.94426	-0.00689	1.03118	0.00456	0.00355	0.00045		
		0.8	0.90436	-0.01007	1.08189	0.01054	0.04524	0.00631		
		0.9	0.88445	-0.00640	1.09778	0.01246	0.17640	0.02714		
		0.95	0.86894	0.00232	1.07220	0.00693	0.4270	0.0743		
		0.97	0.85849	0.01026	1.02641	-0.00371	0.6987	0.1348		
		0.98	0.85097	0.01656	0.9740	-0.0173	0.9721	0.2043		
		0.99	0.8403	0.0260	0.8507	-0.0544	1.571	0.383		
		0.995	0.8326	0.0332	0.6825	-0.1146	2.357	0.666		
		5	0	0.2	0.99911	0.00004	1.00045	-0.20E-4	0.53E-6	-0.15E-6
				0.4	0.99343	0.00014	1.00357	-0.00016	0.78E-4	-0.21E-4
0.6	0.98263			-0.00118	1.01165	-0.00047	0.00171	-0.00044		
0.8	0.98020			-0.01277	1.02295	0.71E-4	0.01982	-0.00484		
0.9	0.99610			-0.03400	1.02103	0.00364	0.06609	-0.01632		
0.95	1.01230			-0.05202	1.00856	0.01007	0.1307	-0.0344		
0.97	1.01437			-0.05464	0.9967	0.0158	0.1800	-0.0502		
0.98	1.00764			-0.04812	0.9874	0.0206	0.2165	-0.0634		
0.99	0.9809			-0.0216	0.9732	0.0284	0.268	-0.085		
0.995	0.9444			0.0148	0.9626	0.0352	0.305	-0.104		
5	5			0.2	0.99803	-0.00013	1.00099	0.66E-4	0.81E-6	0.99E-8
				0.4	0.98514	-0.00104	1.00794	0.00053	0.00012	0.15E-5
		0.6	0.95746	-0.00343	1.02652	0.00178	0.00263	0.38E-4		
		0.8	0.92580	-0.00796	1.05789	0.00422	0.03204	0.00050		
		0.9	0.91218	-0.01020	1.06683	0.00612	0.1155	0.0015		
		0.95	0.90258	-0.00763	1.05184	0.00766	0.2514	0.0023		
		0.97	0.89465	-0.00234	1.0301	0.0089	0.3755	0.0016		
		0.98	0.88762	0.00340	1.0089	0.0099	0.4829	0.0003		
		0.99	0.8752	0.0146	0.9684	0.0121	0.675	-0.004		
		0.995	0.8642	0.0249	0.9263	0.0144	0.869	-0.011		

with the increase in $2a/r_{12}$, but in the opposite directions. As illustrated in figure 4, the direction of rotation of two vesicles undergoing osmophoresis beside each other is different from that of two settling spheres (Goldman *et al.* 1966; Happel & Brenner 1983) or two electrophoretic particles (Chen & Keh 1988; Keh & Chen 1989).

Using a method of reflections, Anderson (1986) obtained the interaction effect for the coupled osmophoretic motion of two identical spherical vesicles with $\kappa = \bar{\kappa} = 0$ oriented arbitrarily with respect to the solute concentration gradient. For the axisymmetric and transverse motions considered here, his results give

$$M_{11}^{(p)} + M_{12}^{(p)} = 1 - 3\left(\frac{a}{r_{12}}\right)^3 + 23\left(\frac{a}{r_{12}}\right)^6 + O\left(\frac{a}{r_{12}}\right)^8 \tag{34a}$$

and

$$M_{11}^{(n)} + M_{12}^{(n)} = 1 + \frac{3}{2}\left(\frac{a}{r_{12}}\right)^3 + \frac{3}{4}\left(\frac{a}{r_{12}}\right)^6 + O\left(\frac{a}{r_{12}}\right)^8. \tag{34b}$$

The values of $M_{11}^{(p)} + M_{12}^{(p)}$ and $M_{11}^{(n)} + M_{12}^{(n)}$ calculated from the above asymptotic solution, with the $O(r_{12}^{-8})$ terms neglected, are also listed in table 3 for a comparison. It can be seen that the

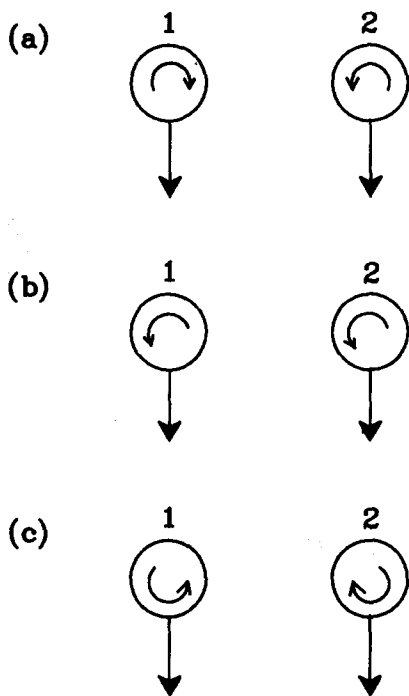


Figure 4. A comparison for the directions of particles' rotation during the motion of two freely suspended spheres perpendicular to their line of centers: (a) sedimentation; (b) electrophoresis; (c) osmophoresis.

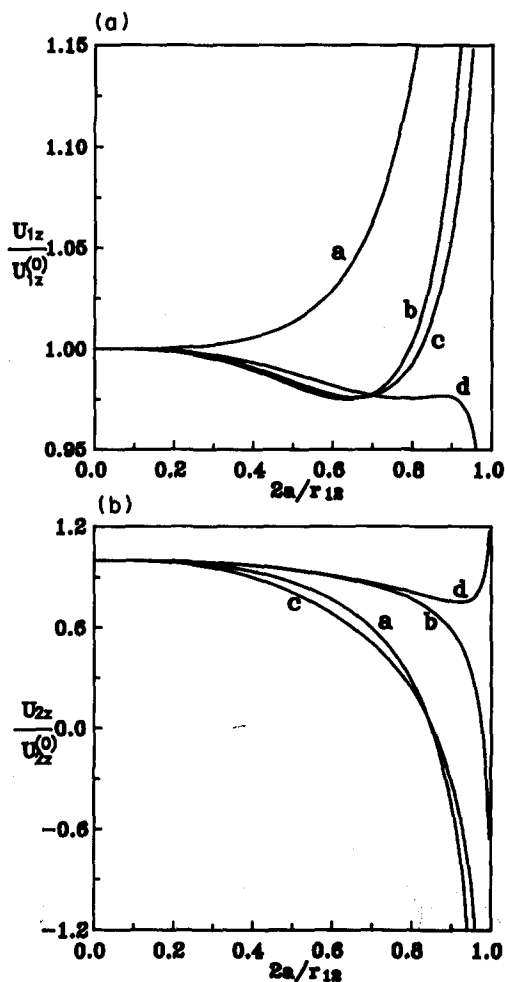


Figure 5. Plots of the normalized velocities of two vesicles of equal radii and hydraulic coefficients undergoing osmophoresis along their line of centers vs the separation parameter $2a/r_{12}$: (a) vesicle 1; (b) vesicle 2. Curve a: $\kappa_1 = \bar{\kappa}_1 = \bar{\kappa}_2 = 0, \kappa_2 = 5$. Curve b: $\kappa_1 = 0, \kappa_2 = \bar{\kappa}_1 = \bar{\kappa}_2 = 5$. Curve c: $\kappa_1 = \kappa_2 = \bar{\kappa}_1 = 0, \bar{\kappa}_2 = 5$. Curve d: $\bar{\kappa}_1 = 0, \kappa_1 = \kappa_2 = \bar{\kappa}_2 = 5$.

asymptotic formulas [34a,b] from the method of reflections agree very well with the exact results as long as the vesicle surfaces are more than 2/3 of the sum of radii apart (i.e. $2a/r_{12} \leq 0.6$). However, accuracy begins to deteriorate, as expected, when the vesicles are closed together (say, $2a/r_{12} \geq 0.8$). Note that [34a] always underestimates the interaction effect between the vesicles and [34b] always overestimates the vesicles' interaction [that means both of their $O(r_{12}^{-8})$ terms must be negative].

The numerical results of the normalized migration velocities for the axisymmetric osmophoresis of two vesicles with equal radii and hydraulic coefficients but different values of κ or $\bar{\kappa}$ are plotted vs $2a/r_{12}$ in figures 5(a,b) with $\kappa_1, \kappa_2, \bar{\kappa}_1$ and $\bar{\kappa}_2$ as parameters. Although these results illustrate that the effect of interactions between the vesicles, in general, increases as the separation distance is decreased, they show that the osmophoretic velocities of the vesicles are not necessarily a monotonic increasing or decreasing function of the separation parameter $2a/r_{12}$. When the two vesicles are very close to each other, the velocity of one is dramatically enhanced from the value it would possess if isolated, while the velocity of the other is greatly reduced from its undisturbed value. Note that, the latter vesicle may even change its direction of movement, as illustrated by curves a, b and c in figure 5(b). Also, curves d in figures 5(a,b), which correspond to low $\bar{\kappa}_1$ and

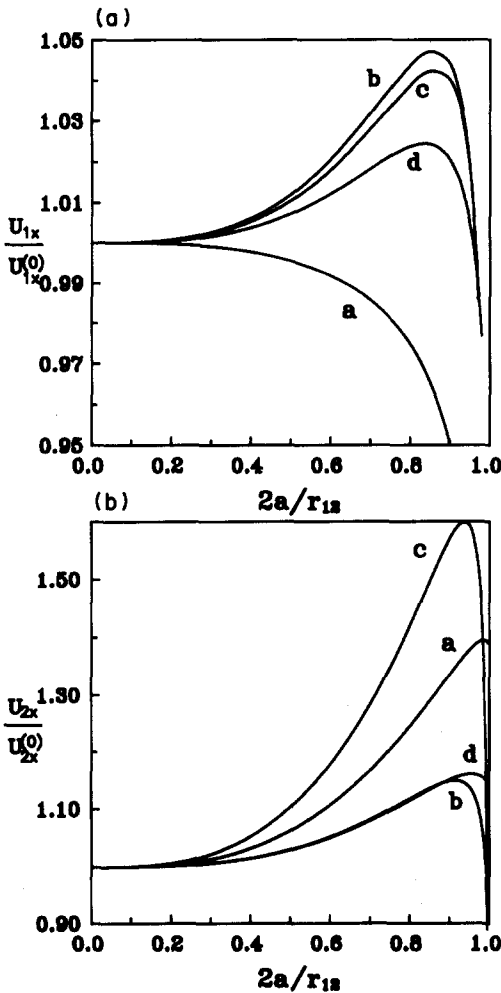


Figure 6. Plots of the normalized translational velocities of two vesicles of equal radii and hydraulic coefficients undergoing osmophoresis perpendicular to their line of centers vs the separation parameter $2a/r_{12}$: (a) vesicle 1; (b) vesicle 2. Curve a: $\kappa_1 = \bar{\kappa}_1 = \bar{\kappa}_2 = 0, \kappa_2 = 5$. Curve b: $\kappa_1 = 0, \kappa_2 = \bar{\kappa}_1 = \bar{\kappa}_2 = 5$. Curve c: $\kappa_1 = \kappa_2 = \bar{\kappa}_1 = 0, \bar{\kappa}_2 = 5$. Curve d: $\bar{\kappa}_1 = 0, \kappa_1 = \kappa_2 = \bar{\kappa}_2 = 5$.

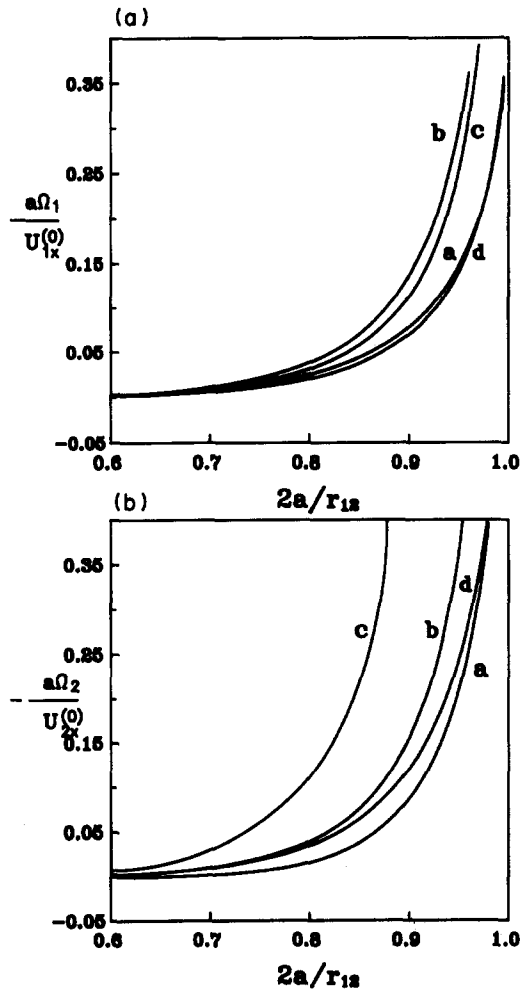


Figure 7. Plots of the normalized rotational velocities of two vesicles of equal radii and hydraulic coefficients undergoing osmophoresis perpendicular to their line of centers vs the separation parameter $2a/r_{12}$: (a) vesicle 1; (b) vesicle 2. Curve a: $\kappa_1 = \bar{\kappa}_1 = \bar{\kappa}_2 = 0, \kappa_2 = 5$. Curve b: $\kappa_1 = 0, \kappa_2 = \bar{\kappa}_1 = \bar{\kappa}_2 = 5$. Curve c: $\kappa_1 = \kappa_2 = \bar{\kappa}_1 = 0, \bar{\kappa}_2 = 5$. Curve d: $\bar{\kappa}_1 = 0, \kappa_1 = \kappa_2 = \bar{\kappa}_2 = 5$.

high κ_1 , κ_2 and $\bar{\kappa}_2$, have a very different trend from the others. These complex results are generated from the combined effects of vesicle interactions on local solute concentration gradients and fluid velocity fields.

In figures 6 and 7, numerical results of the normalized translational and rotational velocities, respectively, of two vesicles with equal radii and hydraulic coefficients but different values of κ or $\bar{\kappa}$ undergoing osmophoresis normal to their line of centers are plotted vs $2a/r_{12}$ with κ_1 , κ_2 , $\bar{\kappa}_1$ and $\bar{\kappa}_2$ as parameters. It can be seen that the effect of interactions between the vesicles, in general, increases as the separation distance is decreased. However, as shown in figures 6(a,b), the translational velocities of the vesicles are not necessarily a monotonic function of $2a/r_{12}$. For a given set of κ_1 , κ_2 , $\bar{\kappa}_1$ and $\bar{\kappa}_2$, the influence of the vesicle interaction as a function of $2a/r_{12}$ on the osmophoretic velocities for the case of large-to-moderate vesicle separations in figures 6(a,b) is opposite to that in figures 5(a,b) for the osmophoresis of two vesicles parallel to their line of centers.

In table 5, numerical results of $M_{11}^{(p)}$, $M_{12}^{(p)}$, $M_{21}^{(p)}$ and $M_{22}^{(p)}$ for the case of the axisymmetric osmophoresis of two vesicles with unequal radii are presented. Again, the vesicles' interaction is stronger (the magnitudes of M_{12} and M_{21} are larger) when they are closer together. The effect of the interaction, in general, is far greater on the smaller of the two vesicles than on the larger one (M_{12} increases and M_{21} decreases significantly with increasing a_2/a_1 for the case of

Table 5. The mobility parameters $M_{11}^{(p)}$, $M_{12}^{(p)}$, $M_{21}^{(p)}$ and $M_{22}^{(p)}$ for the osmophoretic motion of two vesicles with identical hydraulic coefficients but unequal radii

$\frac{a_2}{a_1}$	$\kappa_1 = \bar{\kappa}_1$	$\kappa_2 = \bar{\kappa}_2$	$\frac{a_1 + a_2}{r_{12}}$	$M_{11}^{(p)}$	$M_{12}^{(p)}$	$M_{21}^{(p)}$	$M_{22}^{(p)}$
2.0	0.0	0.0	0.2	0.99764	-0.00474	-0.00059	0.99972
			0.4	0.98183	-0.03766	-0.00444	0.99832
			0.6	0.94600	-0.12683	-0.01309	0.99943
			0.8	0.91556	-0.32704	-0.02768	1.02037
			0.9	0.95619	-0.55456	-0.04603	1.05715
			0.95	1.04951	-0.78549	-0.06967	1.09870
			0.97	1.13154	-0.93990	-0.08795	1.12748
			0.98	1.19434	-1.04546	-0.10153	1.14751
			0.99	1.28552	-1.18613	-0.12095	1.17464
			0.995	1.3507	-1.2800	-0.1349	1.1930
2.0	1.25	2.5	0.2	0.99459	-0.0067	-0.00012	0.99952
			0.4	0.95746	-0.0534	-0.00096	0.99677
			0.6	0.86274	-0.01771	-0.00304	0.99388
			0.8	0.69519	-0.04065	-0.00710	1.00174
			0.9	0.58168	-0.05157	-0.01145	1.01247
			0.95	0.53109	-0.04177	-0.01492	1.01415
			0.97	0.52761	-0.02152	-0.01572	1.00787
			0.98	0.53941	0.00010	-0.01491	0.99897
			0.99	0.5771	0.0419	-0.0106	0.9786
			0.995	0.6235	0.0819	-0.0036	0.9556
5.0	0.0	0.0	0.2	0.99537	-0.00926	-0.00007	0.99997
			0.4	0.96317	-0.07402	-0.00052	0.99986
			0.6	0.87789	-0.25037	-0.00129	1.00056
			0.8	0.72693	-0.61327	-0.00164	1.00449
			0.9	0.64655	-0.94080	-0.00190	1.00888
			0.95	0.63775	-1.21474	-0.00280	1.01277
			0.97	0.66263	-1.38190	-0.00375	1.01526
			0.98	0.68613	-1.49184	-0.00455	1.01701
			0.99	0.7404	-1.6386	-0.0058	1.0195
			0.995	0.7878	-1.7377	-0.0069	1.0212
5.0	0.5	2.5	0.2	0.98479	-0.00153	-0.00003	0.99996
			0.4	0.87858	-0.01223	-0.00019	0.99977
			0.6	0.59175	-0.04112	-0.00059	1.00019
			0.8	0.03112	-0.09559	-0.00130	1.00312
			0.9	-0.38854	-0.12562	-0.00230	1.00553
			0.95	-0.61530	-0.11792	-0.00383	1.00622
			0.97	-0.66924	-0.08881	-0.00515	1.00564
			0.98	-0.65623	-0.05477	-0.00617	1.00458
			0.99	-0.5517	0.0163	-0.0075	1.0017
			0.995	-0.3861	0.0907	-0.0082	0.9981

$\kappa_1 = \kappa_2 = \bar{\kappa}_1 = \bar{\kappa}_2 = 0$, as shown in tables 3 and 5). The motion of the larger vesicle slows down the movement of the smaller one and can even change its direction of migration when the gap between the vesicles becomes small. At the same time, the larger vesicle can be speeded up by the presence of the smaller one (now the insubstantial reverse fluid motion caused by the smaller vesicle can assist the larger vesicle in sucking or in expelling fluid through its membrane), but this effect is weak for the case of a large radius ratio.

The numerical results of $M_{ij}^{(n)}$ and N_{ij} for the case of the transverse osmophoresis of two vesicles of unequal sizes are presented in table 6. In general, the effect of the interaction between vesicles is far greater on the smaller vesicle than on the larger one. The motion of the larger vesicle enhances the velocity of the smaller one. At the same time, the larger vesicle is also speeded up by the presence of the smaller one when the separation distance is large or moderate. When the two vesicles are close together, however, the movement of the larger vesicle can be slowed down by the smaller one (now the reverse fluid motion against the migration of the smaller vesicle drags on the larger one).

Table 6. The mobility parameters $M_{ij}^{(n)}$ and N_{ij} ($i, j = 1$ or 2) for the osmophoretic motion of two vesicles with identical hydraulic coefficients but unequal radii

$\frac{a_1 + a_2}{r_{12}}$	$M_{11}^{(n)}$	$M_{12}^{(n)}$	$M_{21}^{(n)}$	$M_{22}^{(n)}$	N_{11}	N_{12}	$-N_{21}$	$-N_{22}$
$a_2/a_1 = 2, \kappa_1 = \bar{\kappa}_1 = 0, \kappa_2 = \bar{\kappa}_2 = 0$								
0.2	1.00119	0.00237	0.00030	1.00015	0.38E - 6	0.13E - 6	0.24E - 6	0.71E - 6
0.4	1.00950	0.01899	0.00239	1.00118	0.60E - 4	0.21E - 4	0.31E - 4	0.97E - 4
0.6	1.03235	0.06446	0.00811	1.00369	0.00156	0.00062	0.00065	0.00182
0.8	1.07924	0.15775	0.01803	1.00437	0.02452	0.01130	0.00798	0.01708
0.9	1.11678	0.23951	0.01863	0.99439	0.10642	0.05053	0.03341	0.05243
0.95	1.14241	0.30671	0.00439	0.97355	0.26581	0.12513	0.08616	0.10605
0.97	1.15770	0.35003	-0.01639	0.95246	0.43113	0.20097	0.14462	0.15548
0.98	1.17010	0.38221	-0.03895	0.93286	0.5881	0.2724	0.2029	0.1999
0.99	1.19574	0.43507	-0.08936	0.89431	0.9028	0.4154	0.3265	0.2858
0.995	1.2309	0.4875	-0.1542	0.8500	1.2718	0.5839	0.4799	0.3836
$a_2/a_1 = 2, \kappa_1 = \bar{\kappa}_1 = 1.25, \kappa_2 = \bar{\kappa}_2 = 2.5$								
0.2	1.00271	0.00034	0.62E - 4	1.00025	0.43E - 6	0.22E - 7	0.35E - 7	0.74E - 6
0.4	1.02171	0.00269	0.00050	1.00195	0.70E - 4	0.38E - 5	0.48E - 5	0.00010
0.6	1.07357	0.00913	0.00167	1.00617	0.00188	0.00011	0.97E - 4	0.00192
0.8	1.17843	0.02232	0.00370	1.00929	0.03032	0.00188	0.00117	0.01907
0.9	1.26463	0.03384	0.00433	0.99822	0.12953	0.00755	0.00444	0.06261
0.95	1.32856	0.04333	0.00349	0.97152	0.31223	0.01632	0.00980	0.13364
0.97	1.36721	0.04942	0.00244	0.94344	0.4908	0.0232	0.0141	0.2013
0.98	1.39565	0.05381	0.00169	0.91713	0.6518	0.0281	0.0172	0.2625
0.99	1.4435	0.0604	0.0012	0.8659	0.9535	0.0337	0.0202	0.3792
0.995	1.4930	0.0658	0.0023	0.8091	1.275	0.035	0.019	0.507
$a_2/a_1 = 5, \kappa_1 = \bar{\kappa}_1 = 0, \kappa_2 = \bar{\kappa}_2 = 0$								
0.2	1.00232	0.00463	0.37E - 4	1.00002	0.46E - 7	0.16E - 7	0.72E - 7	0.21E - 6
0.4	1.01853	0.03705	0.00030	1.00015	0.87E - 5	0.32E - 5	0.93E - 5	0.28E - 4
0.6	1.06278	0.12524	0.00101	1.00037	0.00030	0.00012	0.00017	0.00049
0.8	1.15452	0.30186	0.00204	0.99961	0.00804	0.00328	0.00157	0.00394
0.9	1.24385	0.44970	0.00102	0.99676	0.05391	0.01903	0.00626	0.01048
0.95	1.33941	0.56655	-0.00438	0.99221	0.18195	0.05492	0.01795	0.01924
0.97	1.42343	0.64020	-0.01226	0.98798	0.3434	0.0940	0.0330	0.0269
0.98	1.5029	0.6944	-0.0211	0.9842	0.5121	0.1315	0.0492	0.0337
0.99	1.6719	0.7829	-0.0418	0.9769	0.8750	0.2067	0.0862	0.0465
0.995	1.8885	0.8707	-0.0691	0.9686	1.317	0.295	0.136	0.061
$a_2/a_1 = 5, \kappa_1 = \bar{\kappa}_1 = 0.5, \kappa_2 = \bar{\kappa}_2 = 2.5$								
0.2	1.00766	0.00077	0.13E - 4	1.00002	0.65E - 7	0.48E - 8	0.13E - 7	0.21E - 6
0.4	1.06085	0.00613	0.00010	1.00018	0.12E - 4	0.94E - 6	0.17E - 5	0.28E - 4
0.6	1.20580	0.02073	0.00034	1.00048	0.00044	0.36E - 4	0.31E - 4	0.00050
0.8	1.49838	0.05033	0.00071	0.99973	0.01136	0.00096	0.00032	0.00409
0.9	1.75213	0.07625	0.00053	0.99639	0.07041	0.00566	0.00140	0.01159
0.95	1.96892	0.09848	-0.00073	0.99025	0.21958	0.01646	0.00414	0.02323
0.97	2.1202	0.1137	-0.0024	0.9839	0.3939	0.0280	0.0074	0.0347
0.98	2.2418	0.1256	-0.0042	0.9777	0.5665	0.0387	0.0107	0.0457
0.99	2.4613	0.1457	-0.0077	0.9651	0.916	0.059	0.017	0.068
0.995	2.7002	0.1659	-0.0113	0.9502	1.317	0.079	0.023	0.094

Table 7. Numerical values of $\{[M_{11}^{(p)} + M_{12}^{(p)}] + 2[M_{11}^{(n)} + M_{12}^{(n)}] - 3\}\omega^{-4}$ as a function of ω and results of α for a suspension of identical vesicles with various values of κ and $\bar{\kappa}$

ω	$\kappa = \bar{\kappa} = 0$	$\kappa = 0, \bar{\kappa} = 5$	$\kappa = 5, \bar{\kappa} = 0$	$\kappa = \bar{\kappa} = 5$
0.0	0.00000	0.00000	0.00000	0.00000
0.1	0.00421	0.00439	0.00240	0.00250
0.2	0.01518	0.01765	0.00295	0.01023
0.3	0.03451	0.03975	0.00844	0.02298
0.4	0.06063	0.07006	0.01481	0.04029
0.5	0.09198	0.10666	0.02217	0.06084
0.6	0.12510	0.14543	0.02937	0.08194
0.7	0.15399	0.17881	0.03424	0.09872
0.8	0.16826	0.19323	0.03287	0.10265
0.9	0.14085	0.15017	0.01743	0.07294
0.95	0.06849	0.03625	-0.00305	0.01710
0.96	0.03728	-0.01635	-0.00943	-0.00435
0.97	-0.00825	-0.09699	-0.01714	-0.03370
0.98	-0.08215	-0.23768	-0.02667	-0.07751
0.99	-0.23381	-0.56349	-0.03889	-0.15555
0.995	-0.4167	-1.0188	-0.0461	-0.2343
1.0	-0.974 ^a	-2.680 ^a	-0.056 ^a	-0.421 ^a
	$\alpha = 3.58$	$\alpha = 2.32$	$\alpha = 3.12$	$\alpha = 2.47$

^aValues evaluated by extrapolation.

Volume fraction dependence of osmophoretic velocity

The interaction effects between pairs of vesicles can be used to determine how the average osmophoretic velocity of suspension is affected by the volume fraction $\bar{\phi}$ of the vesicles. For a bounded suspension of identical vesicles, the mean osmophoretic velocity can be expressed as

$$\langle \mathbf{U} \rangle = \mathbf{U}^{(0)}[1 + \alpha\bar{\phi} + O(\bar{\phi}^2)], \tag{35}$$

with

$$\alpha = 3 - \frac{3}{2} \bar{\kappa} \left(1 + \bar{\kappa} + \frac{\kappa}{2}\right)^{-1} + 8 \int_0^1 \{[M_{11}^{(p)} + M_{12}^{(p)}] + 2[M_{11}^{(n)} + M_{12}^{(n)}] - 3\}\omega^{-4} d\omega, \tag{36}$$

where $\omega = 2a/r_{12}$ and $\mathbf{U}^{(0)}$ is the osmophoretic velocity of an isolated vesicle given by [3] taking $\lambda = 0$. The proof of [35] and [36] is given in the appendix.

The numerical results of the integrand in [36], as a function of ω for various values of κ and $\bar{\kappa}$ computed from the solution of two-vesicle interaction parameters, are exhibited in table 7. The integration can be performed numerically using these data, and the results of the coefficient α are presented in the last row of table 7. Note that, in each case, α is positive and the mean osmophoretic velocity becomes larger when the volume fraction of the vesicles is increased. This behavior, which is different from that for sedimentation (Batchelor 1972), electrophoresis (Anderson 1986) and thermocapillary motion (Anderson 1985), is understandable because the direction of the solvent flow is opposite to that of the vesicles' movement and the back flow of solvent in the bounded suspension enhances the migration of vesicles.

The method-of-reflection solution of the mobility parameters given by [34a,b] can be substituted into [36] to obtain the following analytical formula for α for the case of $\kappa = \bar{\kappa} = 0$:

$$\alpha = \frac{193}{48}. \tag{37}$$

[The expression $\alpha = 121/48$ obtained by Anderson (1986) is probably in error.] Compared with the exact solution given in table 7, the value of α predicted by [37] with $O(r_{12}^{-8})$ terms neglected is about 12% larger.

CONCLUDING REMARKS

The osmophoresis of two arbitrarily oriented spherical vesicles formed from semipermeable membranes has been examined in this paper. The analysis includes two key assumptions: no

boundary deformation and no particle–particle interaction potential; although both phenomena may be important when the vesicles are in close proximity. The solute concentration and fluid velocity fields are solved using bipolar coordinates and the translational and angular velocities of the vesicles are obtained for various values of the system properties, vesicle radii and separation distance. The results indicate that the interaction between vesicles can be strong and peculiar when their gap thickness approaches zero. The translational velocity of two identical osmophoretic vesicles may not be a monotonic function of the separation parameter $2a/r_{12}$, and the direction of rotation of each vesicle is opposite to that for the corresponding motion driven by the gravitational field. The asymptotic formulas [34a,b] derived from the method of reflections for two identical vesicles with $\kappa = \bar{\kappa} = 0$ always give too small an effect of the axisymmetric particle interaction and too larger an effect of the transverse particle interaction, and the error can be significant when the vesicles are nearly in contact. For the case of two vesicles with unequal radii or different values of κ and $\bar{\kappa}$, the particle interaction can be very strong and one vesicle may even change its direction of movement when the vesicles are almost in contact. In general, the effect of the interaction is much stronger on the smaller vesicle than on the larger one. For the special case of two identical vesicles: both migrate with the same velocity, the magnitude of which is smaller for the axisymmetric osmophoresis and larger for the transverse motion (as $2a/r_{12} \lesssim 0.98$) than that which would exist in the absence of the other one.

The interaction effects between pairs of vesicles have also been used to find the mean osmophoretic velocity in a bounded dispersion of vesicles. This mean velocity is enhanced for various cases as the concentration of vesicles in the suspension is increased.

Throughout this work we have assumed that the membranes of the vesicles are semipermeable. For a membrane permeable to the solute species, the osmotic flow is only a fraction of the value expected for a semipermeable membrane, and [1] should be written as

$$v_n = L_p(\sigma \Delta\Pi - \Delta P), \quad [38]$$

where σ is a reflection coefficient. For a semipermeable membrane, $\sigma = 1$; for a non-selective membrane, $\sigma = 0$. For the osmophoresis of a spherical vesicle with an arbitrary value of σ in unbounded fluids, an analytical expression to correct [3] has been obtained (Anderson 1984).

Acknowledgement—Part of this research was supported by the National Science Council of the Republic of China.

REFERENCES

- ANDERSON, J. L. 1983 Movement of a semipermeable vesicle through an osmotic gradient. *Phys. Fluids* **26**, 2871–2879.
- ANDERSON, J. L. 1984 Shape and permeability effects on osmophoresis. *PhysicoChem. Hydrodynam.* **5**, 205–216.
- ANDERSON, J. L. 1985 Droplet interactions in thermocapillary motion. *Int. J. Multiphase Flow* **11**, 813–824.
- ANDERSON, J. L. 1986 Transport mechanisms of biological colloids. *Ann. N.Y. Acad. Sci. (Biochem. Engng IV)* **469**, 166–177.
- BATCHELOR, G. K. 1972 Sedimentation in a dilute dispersion of spheres. *J. Fluid Mech.* **52**, 245–268.
- BERG, H. C. & TURNER, L. 1990 Chemotaxis of bacteria in glass capillary arrays. *Biophys. J.* **58**, 919–930.
- CHARNICK, S. B. & LAUFFENBURGER, D. A. 1990 Mathematical analysis of cell–target encounter rate in three dimensions. *Biophys. J.* **57**, 1009–1023.
- CHEN, S. B. & KEH, H. J. 1988 Electrophoresis in a dilute dispersion of colloidal spheres. *AIChE JI* **34**, 1075–1085.
- DEAN, W. R. & O'NEILL, M. E. 1963 A slow motion of viscous liquid caused by the rotation of a solid sphere. *Mathematika* **10**, 13–24.
- DEVREOTES, P. N. & ZIGMOND, S. H. 1988 Chemotaxis in eukaryotic cells: a focus on leukocytes and dictyostelium. *A. Rev. Cell Biol.* **4**, 649–686.

- GOLDMAN, A. J., COX, R. G. & BRENNER, H. 1966 The slow motion of two identical arbitrarily oriented spheres through a viscous fluid. *Chem. Engng Sci.* **21**, 1151–1170.
- GORDON, L. G. M. 1981 Osmophoresis. *J. Phys. Chem.* **85**, 1753–1755.
- HABER, S., HETSRONI, G. & SOLAN, A. 1973 On the low Reynolds number motion of two droplets. *Int. J. Multiphase Flow* **1**, 57–71.
- HAPPEL, J. & BRENNER, H. 1983 *Low Reynolds Number Hydrodynamics*. Nijhoff, The Hague, The Netherlands.
- KEH, H. J. & ANDERSON, J. L. 1985 Boundary effects on electrophoretic motion of colloidal spheres. *J. Fluid Mech.* **153**, 417–439.
- KEH, H. J. & CHEN, S. B. 1989 Particle interactions in electrophoresis—II. Motion of two spheres normal to their line of centers. *J. Colloid Interface Sci.* **130**, 556–567.
- KEH, H. J. & CHEN, S. H. 1990 The axisymmetric thermocapillary motion of two fluid droplets. *Int. J. Multiphase Flow* **16**, 515–527.
- MEYYAPPAN, M., WILCOX, W. R. & SUBRAMANIAN, R. S. 1983 The slow axisymmetric motion of two bubbles in a thermal gradient. *J. Colloid Interface Sci.* **94**, 243–257.
- MORSE, P. M. & FESHBACH, H. 1953 *Method of Theoretical Physics*, Part II. McGraw-Hill, New York.
- O'NEILL, M. E. 1964 A slow motion of viscous liquid caused by a slowly moving solid sphere. *Mathematika* **11**, 67–74.
- REED, C. C. & ANDERSON, J. L. 1980 Hindered settling of a suspension at low Reynolds number. *AIChE JI* **26**, 816–827.
- STIMSON, M. & JEFFERY, G. B. 1926 The motion of two spheres in a viscous fluid. *Proc. R. Soc. Lond.* **A111**, 110–116.
- WAKIYA, S. 1967 Slow motions of a viscous fluid around two spheres. *J. Phys. Soc. Japan* **22**, 1101–1109.

APPENDIX

The Average Osmophoretic Velocity in a Dispersion of Vesicles

The details of two-vesicle interactions can be used to calculate the mean osmophoretic velocity in a dispersion of vesicles. In this appendix, we obtain formulas for this mean velocity as a function of the volume fraction of the vesicles.

For a bounded suspension, it is no longer possible to define the vesicle velocity relative to the distant fluid, as the vesicles are spread through the entire volume and there is no distant fluid. Instead, the vesicle velocity should be calculated for a reference frame in which the net vesicle and fluid flux is zero and ∇C_∞ is the volume average of the solute concentration gradient field over the entire suspension. Thus,

$$\frac{1}{V} \int_V \mathbf{v}(\mathbf{r}) \, d\mathbf{r} = \mathbf{0} \quad [\text{A.1a}]$$

and

$$\frac{1}{V} \int_V \nabla C(\mathbf{r}) \, d\mathbf{r} = \nabla C_\infty, \quad [\text{A.1b}]$$

where V denotes the entire volume of the suspension.

Based on a microscopic model of particle interactions in a dilute dispersion which involves both statistical and low Reynolds number hydrodynamic concepts (Batchelor 1972; Reed & Anderson 1980), the mean osmophoretic velocity of a “test” vesicle (subscript t), which samples all positions in the bounded suspension, is given by

$$\begin{aligned} \langle \mathbf{U}_t \rangle = & \mathbf{U}_t^{(0)} + N \left\{ \int_V \mathbf{v}^*(\mathbf{r}) [g(\mathbf{r}) - 1] \, d\mathbf{r} - \frac{1}{2} a_t L_{pt} RT \left(1 + \bar{\kappa}_t + \frac{\kappa_t}{2} \right)^{-1} \right. \\ & \left. \times \int_V \nabla [C^*(\mathbf{r}) - C_\infty(\mathbf{r})] [g(\mathbf{r}) - 1] \, d\mathbf{r} + \int_V \mathbf{W}(\mathbf{r}) g(\mathbf{r}) \, d\mathbf{r} \right\} + O(N^2). \quad [\text{A.2}] \end{aligned}$$

Here,

$$\mathbf{U}_i^{(0)} = -\frac{1}{2}a_i L_{pt} RT \left(1 + \bar{\kappa}_i + \frac{\kappa_i}{2}\right)^{-1} \nabla C_\infty, \quad [\text{A.3}]$$

which is the undisturbed osmophoretic velocity of the test vesicle, $g(\mathbf{r})$ is the two-particle radial distribution function and N is the macroscopic concentration of the neighboring vesicles (assumed to have identical values of a , L_p , κ and $\bar{\kappa}$). $C^*(\mathbf{r})$ and $\mathbf{v}^*(\mathbf{r})$ are the solute concentration and fluid velocity fields, respectively, at position \mathbf{r} when a single neighboring vesicle at the origin $\mathbf{0}$ moves due to the external concentration gradient ∇C_∞ , which can be expressed as (Anderson 1983, 1986):

$$r < a: \quad C^*(\mathbf{r}) = \bar{C} + \frac{3}{2} \bar{\kappa} \left(1 + \bar{\kappa} + \frac{\kappa}{2}\right)^{-1} \mathbf{r} \cdot \nabla C_\infty, \quad [\text{A.4a}]$$

$$\mathbf{v}^*(\mathbf{r}) = \left[-5\mathbf{I} + 3\left(\frac{r}{a}\right)^2 (2\mathbf{I} - \mathbf{e}\mathbf{e}) \right] \cdot \mathbf{U}^{(0)}, \quad [\text{A.4b}]$$

and

$$r > a: \quad C^*(\mathbf{r}) = C_\infty(\mathbf{0}) + \left\{ 1 + \frac{1}{2} \left[1 - \frac{3}{2} \kappa \left(1 + \bar{\kappa} + \frac{\kappa}{2}\right)^{-1} \right] \left(\frac{a}{r}\right)^3 \right\} \mathbf{r} \cdot \nabla C_\infty, \quad [\text{A.5a}]$$

$$\mathbf{v}^*(\mathbf{r}) = \left(\frac{a}{r}\right)^3 (\mathbf{I} - 3\mathbf{e}\mathbf{e}) \cdot \mathbf{U}^{(0)}. \quad [\text{A.5b}]$$

(Note that [19a] of Anderson (1983) and [12a] of Anderson (1986) contain typographical errors.) $\mathbf{W}(\mathbf{r})$ is a correction function needed to account for the perturbation on \mathbf{v}^* owing to the presence of the test vesicle, and is defined by

$$\mathbf{W}(\mathbf{r}) = \mathbf{U}_i^*(\mathbf{r}) - \mathbf{U}_i^{(0)} - \mathbf{v}^*(\mathbf{r}) + \frac{1}{2}a_i L_{pt} RT \left(1 + \bar{\kappa}_i + \frac{\kappa_i}{2}\right)^{-1} \nabla [C^*(\mathbf{r}) - C_\infty(\mathbf{r})], \quad [\text{A.6}]$$

where $\mathbf{U}_i^*(\mathbf{r})$ is the actual velocity of the test vesicle located at \mathbf{r} with respect to the origin of a single neighbor at $\mathbf{0}$. One can write

$$\mathbf{U}_i^*(\mathbf{r}) = \underline{\mathbf{M}}_{11} \cdot \mathbf{U}_i^{(0)} + \underline{\mathbf{M}}_{12} \cdot \mathbf{U}^{(0)}, \quad [\text{A.7}]$$

with

$$\underline{\mathbf{M}}_{11} = M_{11}^{(p)} \mathbf{e}\mathbf{e} + M_{11}^{(n)} (\mathbf{I} - \mathbf{e}\mathbf{e}) \quad [\text{A.8a}]$$

and

$$\underline{\mathbf{M}}_{12} = M_{12}^{(p)} \mathbf{e}\mathbf{e} + M_{12}^{(n)} (\mathbf{I} - \mathbf{e}\mathbf{e}); \quad [\text{A.8b}]$$

where subscripts 1 and 2 denote the test and neighboring vesicles, respectively, and the mobility parameters $M_{11}^{(p)}$, $M_{11}^{(n)}$, $M_{12}^{(p)}$ and $M_{12}^{(n)}$ are same as those defined by [31a]. Note that the Faxen correction term involving $\nabla^2 \mathbf{v}^*$, which should have appeared in [A.2] and [A.6], equals zero, as computed from [A.4b] and [A.5b].

To evaluate the volume integrals in [A.2], we assume that the radial distribution function has the following equilibrium value for rigid spheres without long-range pair potential:

$$g = 0 \quad \text{if } r < a_i + a \quad [\text{A.9a}]$$

and

$$g = 1 + O(N) \quad \text{if } r > a_i + a, \quad [\text{A.9b}]$$

where $r = |\mathbf{r}|$ and $O(N)$ is a term proportional to the concentration of neighbors. In other words, the vesicles must be sufficiently small so that Brownian motion dominates any multiparticle hydrodynamic interactions that might impart microscopic structure to the suspension.

Given [A.4a,b] and [A.5a,b] for C^* and \mathbf{v}^* , [A.7] for \mathbf{U}_i^* and [A.9a,b] for g , the integrals in [A.2] are evaluated to obtain

$$\langle \mathbf{U}_i \rangle = \mathbf{U}_i^{(0)} [1 + \alpha \bar{\varphi} + O(\bar{\varphi}^2)], \quad [\text{A.10}]$$

with

$$\alpha = 1 - \frac{3}{2} \bar{\kappa} \left(1 + \bar{\kappa} + \frac{\kappa}{2}\right)^{-1} + 2 \frac{U^{(0)}}{U_i^{(0)}} + \left(1 + \frac{a_i}{a}\right)^3 \times \int_0^1 \left\{ [M_{11}^{(p)} + 2M_{11}^{(n)} - 3] + [M_{12}^{(p)} + 2M_{12}^{(n)}] \frac{U^{(0)}}{U_i^{(0)}} \right\} \omega^{-4} d\omega, \quad [\text{A.11}]$$

where $\omega = (a + a_i)/r$ and $\bar{\varphi} = (4/3)\pi a^3 N$ is the volume fraction of the neighboring vesicles.

Consider now a suspension of vesicles that have a distribution in radius and physical properties. A generalization of [A.10] and [A.11] results in

$$\langle U_i \rangle = U_i^{(0)} \left[1 + \sum_j \alpha_{ij} \bar{\varphi}_j + O(\bar{\varphi}^2) \right], \quad [\text{A.12}]$$

where

$$\alpha_{ij} = 1 - \frac{3}{2} \bar{\kappa}_j \left(1 + \bar{\kappa}_j + \frac{\kappa_j}{2}\right)^{-1} + 2 \frac{U_j^{(0)}}{U_i^{(0)}} + \left(1 + \frac{a_i}{a_j}\right)^3 \times \int_0^1 \left\{ [M_{11}^{(p)} + 2M_{11}^{(n)} - 3] + [M_{12}^{(p)} + 2M_{12}^{(n)}] \frac{U_j^{(0)}}{U_i^{(0)}} \right\} \omega^{-4} d\omega. \quad [\text{A.13}]$$

Here the subscript i denotes vesicles having radius a_i , parameters κ_i and $\bar{\kappa}_i$, undisturbed velocity $U_i^{(0)}$ ($=|U_i^{(0)}|$) and volume fraction $\bar{\varphi}_i$; $\omega = (a_1 + a_2)/r_{12}$; subscripts 1 and 2 of the mobility parameters represents i and j type vesicles, respectively.

In a suspension of identical vesicles, the mean osmophoretic velocity can be reduced from [A.12] and [A.13] to [35] and [36].